M 2014

U.PORTO
FEUP FACULDADE DE ENGENHARIA
UNIVERSIDADE DO PORTO

# DEVELOPMENT AND CHARACTERIZATION OF A CO-CULTURE TWO-DIMENSIONAL BLOOD-BRAIN BARRIER FOR THE STUDY OF NANOPARTICLE PERMEATION

**BÁRBARA BRUNA DA SILVA MENDES**

DISSERTAÇÃO DE MESTRADO APRESENTADA
À FACULDADE DE ENGENHARIA DA UNIVERSIDADE DO PORTO EM
ENGENHARIA BIOMÉDICA

**Faculdade de Engenharia da Universidade do Porto**


# Development and characterization of a co-culture two-dimensional blood-brain barrier for the study of nanoparticle permeation

Bárbara Bruna da Silva Mendes

Dissertação realizada no âmbito do
Mestrado em Engenharia Biomédica

Orientador: Prof. Dr. Bruno Sarmento
Co-orientador: Prof. Dr. Domingos Ferreira

Julho de 2014

# Agradecimentos

O resultado contido nesta tese não seria possível sem um conjunto especial de pessoas que disponibilizaram o seu tempo e o seu conhecimento, a quem desejo ser capaz de agradecer da forma que merecem.

Em primeiro lugar queria deixar o meu obrigado ao professor Bruno Sarmento pela dedicação e tempo disponibilizados na leitura deste documento escrito e nos conselhos partilhados ao longo deste ano. Ao seu grupo de investigação que nas longas reuniões permitiram discussões científicas e troca de conhecimento e dúvidas. Um especial obrigado à Carla por toda a ajuda nas técnicas realizadas no INEB, bem como no apoio no desenvolvimento de diversos protocolos.

Ao professor Domingos e Doutora Cláudia Marques pelo acolhimento recebido no Departamento de Tecnologia Farmacêutica e pelo apoio e partilha de conhecimento na parte laboratorial na fase de aprendizagem. Ao professor Paulo Costa por toda a ajuda na compreensão do uso do software e no princípio teórico dos diversos equipamentos associados ao departamento e a posterior ajuda na discussão de resultados. Ao Joel que, sem dúvida, cedeu o seu tempo e conhecimentos dedicado sempre a ajudar novos alunos, bem como a sua imprescindível ajuda com a logística associada a todo o departamento, na requisição de material bem como na marcação das diferentes técnicas usadas. Um especial obrigado ao laboratório de Química Aplicada, que me ajudaram tanto na parte inicial do uso de equipamentos, bem como na cedência de materiais e reagentes que foram fundamentais para o progresso do meu trabalho laboratorial. Um especial obrigado, à Joana Queiroz, Catarina Moura e Doutora Sofia Costa Lima pela incansável simpatia.

A toda a minha família que nunca duvidou de mim e sempre me deram um incentivo extra para sempre acreditar. À minha querida avó São que é uma das grandes inspirações da minha vida e que me fez gostar tanto de trabalhar na área de Neurociências. Ao meu querido Mário por todo o carinho e confiança que deposita em mim todos os dias, foi um caminho nem sempre fácil mas o teu apoio nunca faltou em nenhuma circunstância.

# Abstract

The most crucial limitation in diagnosis and treatment of the tumor brain is the unique and complicated environment imposed by the central nervous system barriers, mainly due to blood-brain barrier. It can be said that blood-brain barrier is a sort of sanctuary site with unique structural and biochemical properties. In the last decades, nanotechnology has been studied to solve this problem, since nanoparticles present a small size and a large surface area which improves the characteristics of drugs. Specifically, in drug encapsulation and in functionalization for a specific target which minimizes unwanted effects and maximize therapeutic effects.

Therefore, the development of a faithful *in vitro* cell system, which would reflect as many relevant *in vivo* BBB properties as possible, it is an important first step in the evaluation of new drugs and new drug delivery systems to cross this barrier. Here, it is purpose a human cell model of the blood brain barrier for use as tool for screening nanoparticles interactions, with emphasis to camptothecin loaded in solid lipid nanoparticles.

In this system, a triple co-culture was established. Endothelial cells were grown in the luminal side of the semi-permeable filter, astrocytes on the inverted side of the insert and a glioma cell line on the bottom of the abluminal side. First, permeability to three different well-known compound showed that endothelial monolayer, besides the lower trans-endothelial electrical resistance values, mimic a highly restrictive barrier. Also, immunocytochemistry and scanning electron images showed a confluent endothelial monolayer at $7^{th}$ day and $4{,}6x10^4$ cells/$cm^2$ initial concentration. On the same day, astrocytes were co-cultured and on $2^{nd}$ a glioma cell line at the same endothelial cell proportion was added. When glioma cell line was added to the *in vitro* model, endothelial cells co-cultured with astrocytes, it is clear the barrier disruption, by decreasing of trans-endothelial electrical resistance values and for scanning electron images it is possible analyze the loss of tight junctions. Finally, the addition of astrocytes is inconclusive because of cellular concentration limitation, however the

astrocytes on scanning electron images seems can influence endothelial monolayer by mechanical forces.

In parallel, it were developed camptothecin loaded in solid lipid nanoparticles as an anti-cancer model drug. The pharmacokinetic properties of camptothecin are not favorable to its free administration, since the compound has low water solubility and is chemically unstable, only at acidic pH has anti-cancer activity. So, incorporation of camptothecin within the hydrophobic matrix is essential to protect the drug from degradation, to increase the therapeutic effect.

The work done before for our group it was accurate and it was established new conditions to produce and characterize these nanoparticles. Solid lipid nanoparticles loaded with camptothecin were produced and characterized. The size around 200 nm, the charge slightly negative and association efficiency values are suitable for cell membrane passage and uptake under normal physiological conditions. Then, the nanoparticles were tested on the three different cells used on the *in vitro* model. Camptothecin loaded in solid lipid nanoparticles consistently showed higher potency as compared to the free camptothecin and low cytotoxicity. Also, it showed more biocompability with endothelial cells that with the astrocytoma cell line.

Therefore, it is necessary analyze nanoparticles permeation on the *in vitro* model and compare those results with the *in vivo*. However, it is expected that the triple co-culture model purposed is a good alternative to screening nanoparticles formulations and can be a new insight to study blood brain barrier structure and mechanisms.

**Keywords:** *In vitro* model, Blood-brain barrier, Camptothecin, Glioma

# Resumo

A baixa eficácia no diagnóstico e no tratamento do tumor cerebral tem como principal razão os complexos mecanismos presentes no sistema nervoso central, especificamente presentes na barreira hemato-encefálica. Atravessar esta barreira torna-se numa tarefa quase impossível principalmente devido às células presentes e aos fatores químicos e biológicos envolvidos. Recentemente, a nanotecnologia tem sido uma área de investigação de grande interesse, uma vez que as nanopartículas apresentam um tamanho reduzido e uma grande área superfície-volume, o que pode melhorar a eficácia terapêutica.

Desta forma, o desenvolvimento de um sistema celular *in vitro*, que apresente o maior número de propriedades *in vivo,* sem dúvida é o primeiro passo para a avaliação de novos medicamentos que necessitam de atravessar a barreira hemato-encefálica. Com o objetivo de aumentar a compreensão das interações presentes nesta barreira e os efeitos das células cerebrais com as nanopartículas é proposto o desenvolvimento de um modelo celular humano da barreira hemato-encefálica e o estudo da camptotecina encapsulada em nanopartículas lipídicas sólidas.

Neste modelo, um sistema de tripla co cultura é estabelecido. As células endoteliais foram colocadas no lado apical da membrana, os astrócitos no lado contrário da membrana no lado basolateral e o glioma no fundo da placa também no lado basolateral. Estudos de permeabilidade com três diferentes moléculas demonstram que a monocamada endotelial, apesar dos baixos valores de resistência elétrica trans endotelial, consegue mimetizar uma barreira selectiva como acontece na situação *in vivo*. Também, as imagens de imunocitoquímica e de microscopia electrónica é possível observar uma monocamada confluente ao sétimo dia e com uma concentração inicial de $4{,}6 \times 10^4$ cells/cm$^2$. Quando, a linha cellular de glioma é adicionada ao modelo torna-se clara a disrupção da barreira pela dimuição dos valores de resistência elétrica trans endotelial e pelas imagens de microscopia electrónica onde é possível observar a perda das ligações características das células

endoteliais. Por último, aquando da adição dos astrócitos os resultados foram inconclusivos devido à limitação celular das células primários, porém através da microscopia electrónica torna-se evidente uma influência mecânica dos astrócitos com as células endoteliais.

Em paralelo foram desenvolvidas nanopartículas incorporados com camptotecina como fármaco anti-cancerígena modelo. As propriedades farmacocinéticas da camptotecina não são favoráveis à sua administração em fármaco livre, uma vez que o fármaco apresenta uma baixa soubilidade em água e apresenta uma estrutura química instável, só a pH ácido é que apresenta actividade anti-cancerígena. Desta forma, a incorporação do fármaco numa matriz hidrofóbica é essencial para proteger a camptotecina da degradação e assim aumentar a eficácia terapêutica.

O trabalho desenvolvido anteriormente pelo nosso grupo com este fármaco foi melhorado e novas condições de produção e caracterização foram desenvolvidas. As nanopartículas com o fármaco incorporado apresentaram tamanhos cerca dos 200nm e carga ligeiramente negativa, o que está de acordo com passage da membrane cellular e a incorporação em condições fisiológicas normais. Posteriormente, as nanopartículas foram testadas nas células usados no modelo cellular. As nanopartículas sem fármaco em todas as condições apresentam baixa citotoxicidade. Por outro lado, a camptotecina livre apresenta a citotoxicidade mais elevada em todas as condições. A camptotecina incorporada nas nanopartículas apresenta uma maior eficácia em comparação com o fármaco livre, e apresenta uma maior biocompatibilidade nas células endoteliais do que com a linha celular de glioma.

Assim sendo, é necessário analisar a permeabilidade das nanopartículas no modelo *in vitro* e comparar os resultados com modelos *in vivo*. Porém, é esperado que o modelo proposto é uma boa alternativa para avaliar novos fármacos incorporados em diferentes sistemas e pode ser uma nova estratégia para estudar a estrutura e mecanismos associados à barreira hemato-encefálica.

**Palavras-chave:** Modelo i*n vitro*, Barreira hemato-encefálica, Camptotecina, Glioma

# Contents

# List of Figures

# Acronyms

| | |
|---|---|
| ABC | Adenosine triphosphate-Binding Cassete |
| AET | Active Efflux Transporter |
| AMT | Absorptive-Mediated Trancytosis |
| BBB | Blood-Brain Barrier |
| BCRP | Breast Cancer Resistance Protein |
| bEnd3 | Immortalized mouse Endothelial cells |
| bFGF | basic Fibroblast Growth Factor |
| BSA | Bovine Serum Albumin |
| CMT | Carrier-Mediated Transport |
| CNS | Central Nervous System |
| CPT | Camptothecin |
| CPT-SLN | Camptothecin-loaded SLN |
| DIV-BBB | Dynamic In vitro Blood-Brain Barrier |
| DLS | Dynamic Light Scattering |
| DMEM | Dulbecco's Modified Eagle's Medium |
| DMSO | DimethylSulfOxide |
| DPBS | Dulbecco's Phosphate Buffered Saline |
| EC | Endothelial Cells |
| EDTA | EthyleneDiamineTetraacetic Acid |
| FBS | Fetal Bovine Serum |
| FD | Fluorescein isothiocyanate – Dextran |
| hCMEC/D3 | human Capillary Endothelial cells |
| HPLC | High Performance Liquid Chromatography |
| HPLC | High Performance Liquid Chromatography |
| JAMS | Junctional Adhesion Molecules |
| MDR | Multidrug Resistance Proteins |
| MRP | Multidrug Resistance-associated Proteins |
| NVU | NeuroVascular Unit |
| P-gp | P-glycoprotein |

| | |
|---|---|
| RMT | Receptor-Mediated Transcytosis |
| SEM | Scanning Electron Microscopy |
| SLN | Solid Lipid Nanoparticles |
| TEER | Trans-Endothelial Electrical Resistance |
| TJ | Tight Junctions |
| WGA | Wheat Germ Agglutinin |
| ZO | Zonula Occludens |

# Chapter 1

# Introduction

The most crucial limitation in diagnosis and treatment of the neuronal diseases is the unique and highly controlled microenvironment of the Central Nervous System (CNS) barriers [1-4]. There are three key interfaces at which cells form barriers between the blood and the CNS, namely the Blood-Brain Barrier (BBB), blood cerebrospinal fluid barrier and the arachnoid barrier [5], being BBB the most important. This interface is formed by specialized endothelial cells (EC) in close association with basement membrane and neighboring cell types within the neurovascular unit [6]. The microvascular endothelium at the BBB is characterized by the presence of tight junctions between adjacent EC, lack of fenestrations, and minimal pinocytotic vesicles [7].

Besides the delivery of drugs to CNS through BBB being really poor and the treatment inefficient, the drugs used present many limitations such as side effects and bioavailabitity. Therefore, it is necessary to develop drug carriers to improve the effects in diagnostics, therapy and theragnostics [8]. The development of a close in vitro cell system is a difficult task and an important first step in the evaluation of new drugs and drug delivery systems to cross the BBB [9]. However, at present, no *in vitro* model can faithfully reproduce all the properties and characteristics of the *in vivo* BBB model.

This chapter will focus on BBB structure and mechanisms. Firstly, its importance functional and morphological it will be analyzed. A brief description of the different types of transporters it will be discussed, as the different techniques to perform brain drug targeting and the current strategies. Finally, it will be present various *in vitro* models divided into static and dynamic ones.

# 1. Blood Brain Barrier

In 1885, more than 120 years ago, Paul Ehrlich was the first to demonstrate the presence of a barrier between blood and brain. He found that intravenously injected dyes, rapidly contrast all organs except the brain [10]. A few years later, his student Edwin Goldman made other experience where he injected these dyes into the cerebrospinal fluid. He found that this route had free access to neural tissue, however not of the peripheral organs. So, these dyes were prevented from directly entering the blood supply of the brain [2]. Since this crucial discovery, our understanding of the BBB molecular structure, physiological processes and our knowledge in its transporters increased [1].

BBB is regarded as an active, dynamic and extremely complex interface between the blood and the CNS which has specific structural and biochemical properties [9]. It is clear that BBB is very important in the protection of neurons from fluctuations in the plasma component and it was the main factor that leads to its development. This interface controls the rate of influx and efflux of biological substances needed for the brain metabolic processes and neuronal function. Because, of its selectivity, the BBB plays a crucial role to regulate the trafficking between blood and CNS and the determination of neuroimmunology and neuropathology [11]. So, BBB provides protection against many toxic compounds and pathogens. For this reason, it is of paramount importance in regulating the constancy of the brain internal environment [9]. It also contributes to ion homeostasis function which keeps the ionic composition optimal for synaptic signaling and preserves neural connectivity. It allows immune surveillance and responses to minimal inflammation and cell damage [5, 12].

Morphologically, the BBB is formed by specialized EC, paving the luminal side (the blood capillary side) in close association with basement membrane and neighboring cell types, which include perivascular pericytes, astrocytes, neurons and microglia in the abluminal membrane. These various cell types and basal lamina collectively constitute the neurovascular unit (NVU), Figure 1 [13]. Other important characteristic of *in vivo* BBB is the shear stress over the surface of the cells which is a tangential force generated by the blood flow [14]. Shear stress promotes the differentiation process and maintenance of BBB phenotype [15].

Specifically, the basement membrane of the cerebral endothelium is constituted by three apposed layers, made of different types of extracellular matrix classes of molecules such as collagen IV [16], glycoproteins, proteoglycans, laminin and various types of matrix adhesion receptors. In adults his membrane is about 30-40 nm thick and separates ECs and pericytes from the surrounding extracellular space [17]. Their interconnections produce a complex matrix which anchors cells and establishes the support for neighboring cells [18]. Also, the neighboring cells play an important role improving the barrier functions. It is a fact that ECs

are the major cellular constituent of the brain. The principal features associated with BBB ECs which differ these cells from the other ones in the rest of the body are the lack of fenestrations, low level of pinocytic vesicles, a high mitochondrial content, the presence of more extensive tight junctions (TJ) with electrical resistance as high as 8000 Ohmcm$^2$ and the expression of various transporters that influence molecule transport to the brain [19]. Concerning to astrocytes, they constitute nearly half of brain cells [20] and encircle 90% of the BBB endothelium on the abluminal side. Astrocytes have a key feature on the induction and maintenance of BBB integrity, namely by the secretion of factors such as transforming growth factor-β, glial-derived neurotrophic factor, basic fibroblast growth factor (bFGF) and angiopoetin 1 into the medium; alter the expression of drug transporters such as P-glycoprotein (P-gp) and induce tighter TJ [21]. Although this importance has been documented since two decades, the molecular pathways still remains unclear [5, 18]. As referred to pericytes, also known as vascular smooth muscle cells, they have a physical association with the endothelium. The release of ECs factors can induce migration of pericytes and affect the maintenance of the integrity of the vessel. Pericytes are able to control the capillary diameter, due to their contractile characteristics, then modulate the cerebral blood flow [22]. Regarding to microglia cells, the exact mechanisms of how microglia influences BBB properties are still unknown, however it is clear that they are playing an important role in immune response and consequently in the BBB integrity [22]. So far, very few are known about the precise role that neurons play on the BBB phenotype. Although, there are some evidence that neurons affect cerebral blood flow and can regulate the function of blood vessels [7].

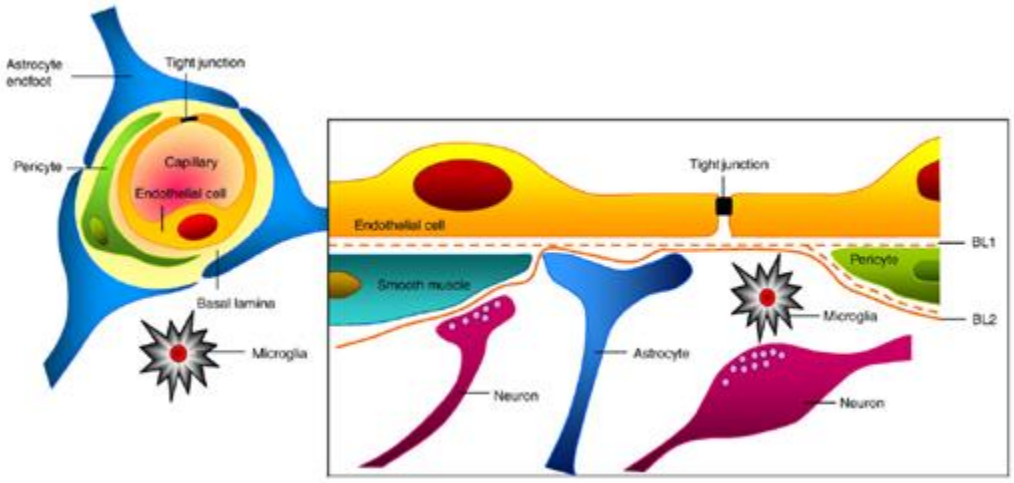


**Figure 1.1** The cell associations at the BBB [5]. The NVU is a complex cellular system that includes highly specialized endothelial cells, a high concentration of pericytes embedded in the endothelial cell basement membrane; astrocytic endfeet associated parenchymal basement membrane, neurons and immune cells. Considering all cellular interactions presents on neurovascular unit, it can be said that BBB presents unique structural and biochemical properties.

TJ consist of an extreme complex of integral proteins spanning the intercellular cleft (occludin and claudins), junctional adhesion molecules (JAMs) and cytoplasmic accessory proteins (zonula occludens (ZO) -1, -2, -3 and cingulin) bound to the actin cytoskeleton, Figure 2. Specifically, claudins form the primary seal of TJ forming dimmers and bind homotypically to claudins on adjacent cells, the level of claudin expression determines TJ integrity. Occludins are the dynamic regulatory protein responsible on TJ regulation, to enhance the transendothelial electrical resitance (TEER) and restrict the paracellular permeability. Together, claudins and occludins form the extracellular component of TJs and are both required for formation of the BBB. And JAMs can regulate the leukocyte migration and it is involved in cell-to-cell adhesion [21]. Basically, ZO proteins serve as recognition proteins for TJ placement and as support structure for signal transduction proteins [17]. In case of adherens juntions, they are located near the basolateral side of ECs. Cadherin proteins span the intercellular cleft and are linked into the cell cytoplasm. The principal function of these junctions is holding the cells together giving the tissue structural support [13]. TJ and AJ components are known to interact and influence TJ assembly [19].

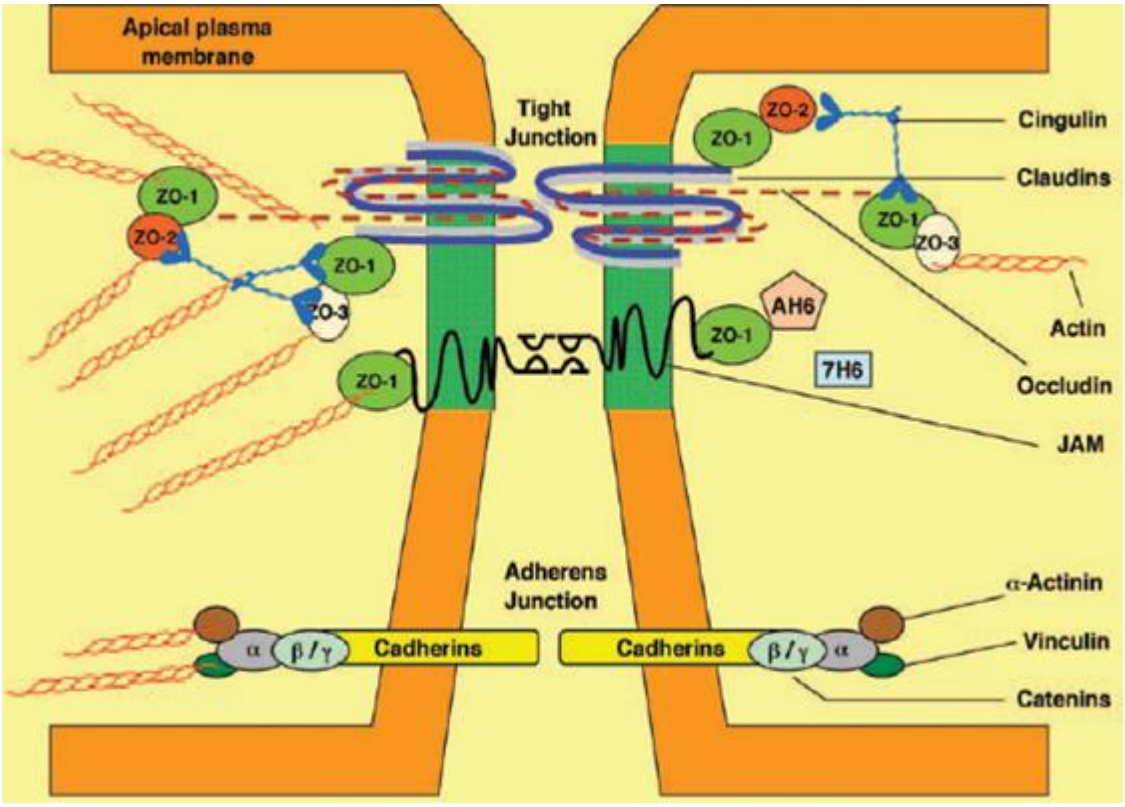


**Figure 1.2** Simplified explanation of the molecular composition of endothelial TJ at the BBB are shown [17]. Three integral proteins form the TJ structure: claudins, occludins and JAM. Claudins produce the primary seal of TJ. Occludin function as a dynamic regulatory protein and JAMs are important to regulate leukocyte migration. TJ consists of accessory proteins such as ZO. All this mechanisms are important to improve the BBB tightness and to reduce the compounds that can cross the BBB.

# 2. Transports across the BBB

With regard to BBB, it can be said that it is a sort of sanctuary site as it strictly controls the exchanges between the blood and brain compartments [8]. As far as small molecule drugs are concerned, more than 98% cannot enter the brain [23]. Consequently, crossing the BBB is a great challenge.

Nonetheless several transporters have been established by means of which solute molecules move across BBB. The various systems that mediate the transport across BBB can be divided into three categories - small molecule, large molecule and efflux transporters (figure 1.3 and 1.4). Within the small molecule transporters there are two possibilities, the diffusion transport and the carrier-mediated transport (CMT). In the first, the passage of molecules across the EC of the BBB can occur between adjacent cells (the paracellular pathway) or through the cells (the transcellular pathway) [7]. Active efflux transporter (AET) is another type of route. Among them the most extensively characterized is adenosine triphosphate-binding cassete (ABC) transporter family. Macromolecule transporters include receptor-mediated transcytosis (RMT), absorptive-mediated transcytosis (AMT) and cell-mediated-transcytosis. This last one refers only to immune cells transport [12].

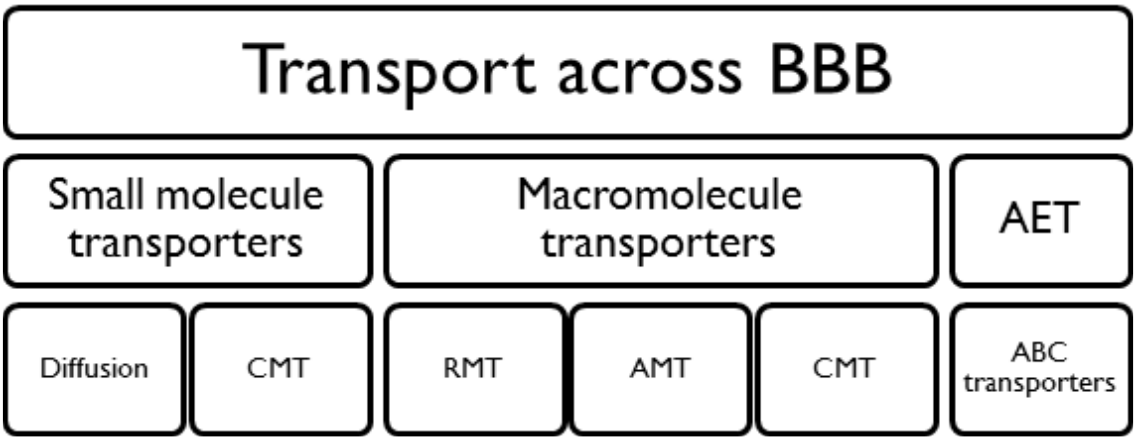


**Figure 1.3** Different type of blood brain barrier (BBB) transporters adapted from [8]. The scheme is divided into three large groups. The first group is about small molecule transporters. The second group is about macromolecule transporters. And the last group is about active efflux transporters (AET). Each group is divided in various small groups which have different biologic and physical characteristics – diffusion and carrier-mediated transport (CMT); receptor-mediated transcytosis (RMT); adsorptive-mediated transcytosis (AMT) and cell-mediated transytosis (CMT); adenosine triphosphate-binding cassete (ABC) transporters.

## 2.1. Small molecule transporters

Within the small molecule transporters there are two possibilities, the diffusion transport – either simply diffusion or facilitated transport across aqueous channels – and the active transport which is mediated by a carrier such as proteins. In the first, the passage of

molecules across the ECs of the BBB can occur between adjacent cells (the paracellular pathway) or through the cells (the transcellular pathway) [8].

With regard to transcellular transport, Lipinski and co-researchers developed five rules that determine if a compound is more likely to be membrane permeable and easily absorbed by the body [24]. In order to achieve his goal, Lipinski analyzed the physicochemical properties of more than 2000 drugs and candidate drugs in clinical trials. His work resulted in the establishment of five criteria that must be fulfilled by the compounds. These are: no more than five hydrogen bond donors (nitrogen or oxygen atoms with one or more hydrogen atoms); no more than ten hydrogen bond acceptors (nitrogen or oxygen atoms); a molecular mass lower than 500 Da; an compound's lipophilicity, expressed as a quantity known as logP (the logarithm of the partition coefficient between water and 1-octanol) lower than 5, and compound classes that are substrates of biological transporters are exceptions to the rule [24]. It is important to state that the rule of five applies only to absorption by passive diffusion of compounds through cell membranes; compounds that are actively transported through cell membranes by transporter proteins are exceptions to the rule. Therefore, it is of limited significance nowadays [23]. However, it is clear that if the molecular weight of a drug molecule is higher than 400 Da or the drug forms more than eight hydrogen bonds, the probability of crossing the blood-brain barrier via passive diffusion in pharmacologically significant amounts is very low [12].

Even though the paracellular transport of hydrophilic substances is virtually absent due to the unique properties of the TJs, small lipid soluble substances, like alcohol and steroid hormones, penetrate transcellularly by dissolving in their lipid plasma membrane [13]. In brief, the paracellular transport is a passive movement of a molecule through the aqueous route of the intercellular cleft between EC via small pores or flaws in the tight junctions. It represents a central functional component of BBB regulation [7].

The relationship between the paracellular and transcellular permeability is the key feature in the regulation of overall trans-endothelial permeability in the endothelium [25].

Concerning to CMT, the active transport is an important transporter that carriers essential polar nutrients to cross the brain namely as glucose, amino acids, and purine bases. This type of route uses carriers, that is to say, membrane-restricted systems commonly involved in the transport of small molecules with a specific size and a molecular weight smaller than 600 Da [8]. The solute carriers may be bi-directional, in which case the direction of net transport is determined by the substrate concentration gradient; unidirectional either into or out of the cell; or involve an exchange of one substrate for another; or be driven by an ion gradient depending on electrochemical gradients. It is also a fact that CMT is substrate selective, considering that the transport rate depends on the degree occupation of the carrier.

Considering that glucose is the main energy source of the brain, glucose transporter-1 plays a vital role within the transporters. Since the density of glucose transporter-1 at the abluminal membrane is higher than at the luminal, there is a homeostatic control for glucose influx into the brain [13, 25].

## 2.2. Macromolecules transporters

Transcytosis of macromolecules across the BBB via endocytotic mechanisms provides the main route by which large molecular weight solutes such as proteins and peptides can enter the CNS intact. Macromolecule transporters include RMT, AMT and CMT.

Extensive studies of RMT have revealed that it offers selective uptake of many different types of ligands, namely plasma proteins, enzymes and growth factors [8], RMT occurs in three steps, first the endocytosis of macromolecules specially bound to a receptor on the endothelial surface of BBB, followed by diffusion across the endothelium, and exocytosis on the opposite site. ECs comprise different receptors, such as transferrin receptor [26], insulin receptor [27], lipoprotein receptors [28], and insulin-like growth factors [27]. Regarding insulin molecules, the ligand first binds to the receptor present at specialized areas of plasma membranes called coated pits. Once bound to ligand, these coated pits invaginate into the cytoplasm and form coated vesicles. The ligand is dissociated from receptor by acidification of endosome and crosses to the other side of the membrane [23].

AMT, also known as pinocytosis, is mediated by electrostatic interaction between positively charged substrates and the negatively charged plasma membrane (i.e. heparin sulphate proteoglycans) [12]. It is important to state that this process does not involve specific plasma membrane receptors. Normally, endocytosis occurs upon binding of the cationic compound to the plasma membrane. In order to protect the brain from nonspecific exposure to polycationic compounds, this vesicular transport is actively downregulated in the BBB [23].

Recently, a new transporter was identified which is based on transport of immune cells (like monocytes or macrophages) to cross the intact BBB [23]. CMT can transport any type of molecules or materials and particulate carrier systems, whereas other mechanisms normally permit only solute molecules with specific properties.

## 2.3. Active efflux transporters

As opposed to the above described influx routes, the efflux transporters play a different role. It is a fact that they can be considered a "first line of defense", since it is up to them to remove xenobiotic molecules and brain potentially neurotoxic endogenous from the brain tissue back into the circulation. In addition, they can significantly restrict the entry of substrate into brain parenchyma. Up until now, the most extensively characterized efflux transporter proteins at BBB is the ABC transporter family [29, 30]. In humans they are a

superfamily of proteins containing 48 members which are grouped into 7 sub-families, ABC A to G. Among the large number of ABC transporters, only three of them are expressed at the blood-brain barrier. The ABCB sub-family contains the multidrug resistance proteins (MDR) of which P-glycoprotein (P-gp) is the best-known representative, the ABCC subfamily contains the multidrug resistance-associated proteins (MRP) and ABCG sub-family contains breast cancer resistance protein (BCRP) [31].

Regarding to the P-gp, it is a membrane-bound protein (170 kDa) which is present at high concentrations in the luminal membrane of the blood-brain barrier endothelium. P-gp has a high affinity for a wide range of cationic and lipophilic compounds and therefore limits the transport of many drugs, including cytotoxic anticancer drugs, antibiotics, hormones, and HIV protease inhibitors. At present, P-glycoprotein is considered the most prominent element of selective barrier function that limits xenobiotics from entering the brain [31].

MRP transports mainly organic anions, glutathione, glucuronide- or sulfateconjugated compounds, as well as various nucleoside analogs. Thus it acts as an organic anion transporter while it also transports neutral organic drugs. MRP transporters have five isoforms present in BBB and BCSFB.

Another BBB efflux transporter is BCRP, which appears to be expressed in the luminal membrane of the cerebral EC in a similar manner to p-glycoprotein. Recent studies suggest some cooperation between BCRP and p-glycoprotein inasmuch as they limit xenobiotics from entering the brain and compensate one another [23]. Four vital reasons justify the need to understand the regulation of these transporters. First of all, it is not known how barrier properties can be altered through environmental factors. Second, inflammatory and oxidative stress seems to affect ABC transporter expression in other barrier and excretory tissues. Third, it is crucial to find out how specific CNS diseases alter transporter function. Finally, it is necessary to discover how ABC transporter-specific inhibitors can improve drug delivery [31].

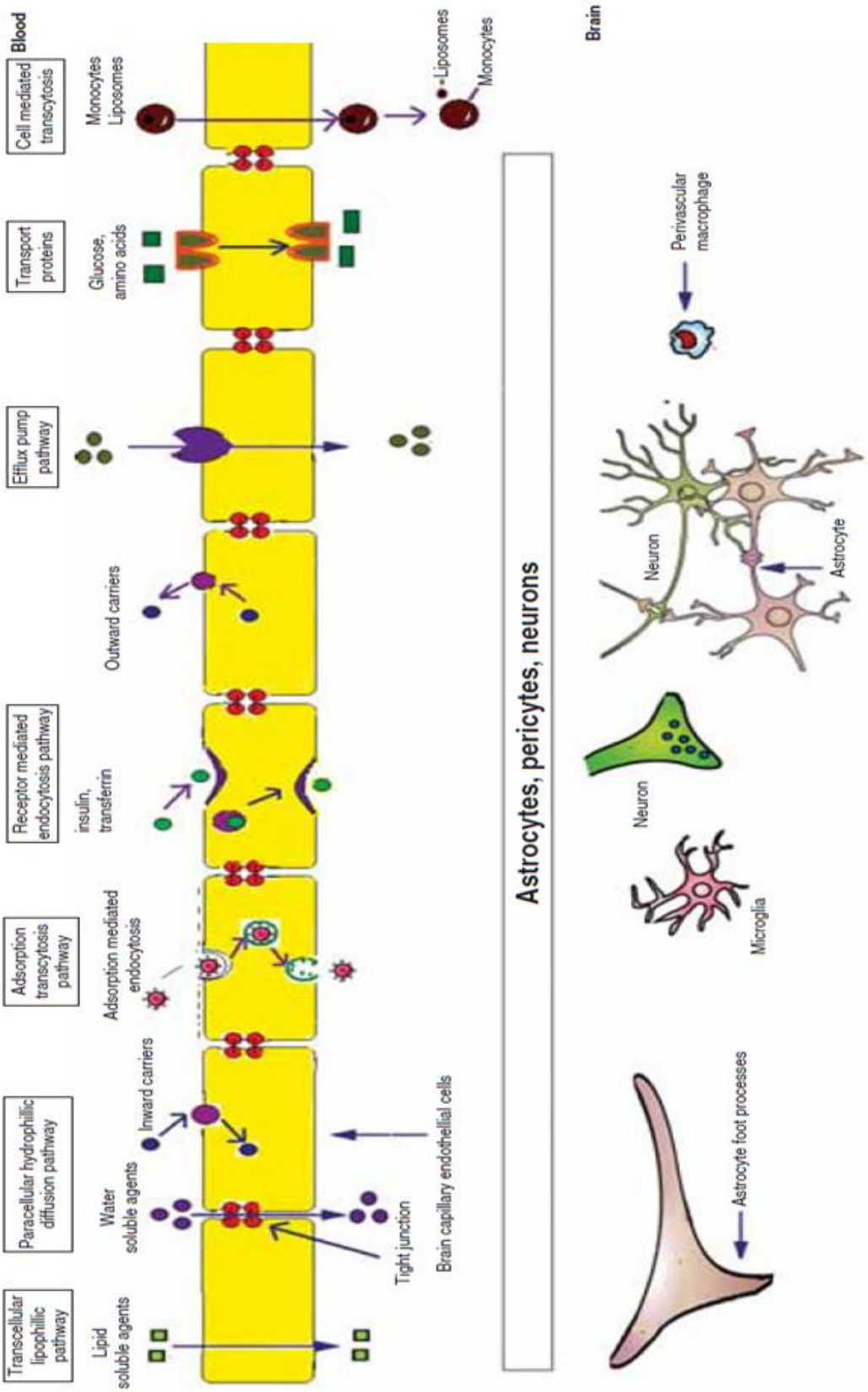


**Figure 1.4** Mechanisms of transport across BBB [22]. This figure explains the involved mechanism of each BBB transporter.

# 3. Drug targeting to the brain

As said before, the most limiting factor in the development of new strategies of diagnosis and therapeutics is the crossing of the BBB. To overcome these limitation, innumerous strategies has been studied to improve the pharmacological quantity that it is able to improve therapeutic efficiency.

Firstly, it will be discuss various routes including direct delivery to CNS and direct systemic delivery. Then, it will be focus in noninvasive approach, namely it will be discussed physiological strategies such as transporter mediated delivery; chemical ones using as example cationic proteins; conjugation of drugs with antibodies is a biological strategy and the various colloidal carrier systems. Figure 1.5 shows a systematic classification of various approaches.

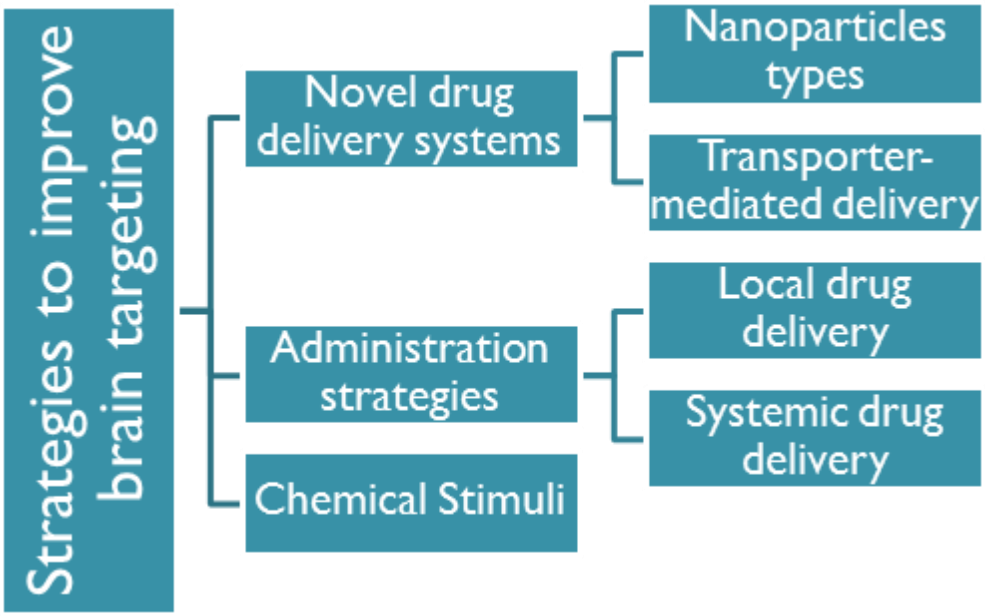


**Figure 1.5** Overview of different strategies for brain targeting of drugs adapted from[23]. Various strategies can be used to improve diagnostic and therapeutic – such as invasive ones (systemic and local drug delivery), and drug delivery strategies which are modified according to the purpose.

## 3.1. Novel drug delivery systems

In this field nanotechnology has been a key feature since it improves the characteristics of different agents [32]. Nanotechnology is the creation and use of functional materials with at least one characteristic dimension measured in nanometers (scale =$10^{-9}$). In this technology unique phenomena enable novel applications because nanosystems have new properties such as large surface-volume ratio, surface charge, small and controlled size. The small size of the nanoparticles enables them to penetrate the BBB and facilitates drug delivery across the barrier [33]. They have large surface-volume ratio resulting in an increase of local interaction

and thereby increasing the rate of dissolution. At the same time, it is possible to do surface functionalization (to improve shelf-life) and to use them as drug carriers (to increase drug bioavailability). They allow for controlled and slow drug release in the brain, while decreasing peripheral toxicity and side effects [23].

Several colloidal system have been studied to improve the BBB crossing such as immunolipossomes [34], Solid Lipid Nanopaticles (SLN) [35], poly(butyl cyanoacrylate) (PBCA) nanoparticles, chitosan nanoparticles, albumin nanoparticles [36].

Functionalization of nanocarriers is one of the most important steps or challenges in formulating nanocarriers for drug delivery. There are two forms the passive or/and active targeting. The passive targeting depending of tissue characteristics like the enhanced permeability and retention on many types of tumors [36]. However, in case of human brain diseases has not been shown to be effective. The advantage of active targeting is the increase of the amount of drug in the target tissue, thereby increasing the pharmacological response and reducing systemic side effects [8]. For example, in the case to increase time of nanoparticles in the organism and drug bioavailability is necessary use active targeting by coating the surface with polyethylene glycol or surfactants like polysorbate 80. Because, if the nanoparticles are unmodified, they rapidly are adsorb, mainly by opsonins, and eliminate for the organism by the macrophages of the reticuloendothelial system [36].

The blood-to-brain transport system is of considerable interest in drug delivery for targeting of drug molecules into brain whereas peptides and small molecules may use specific transporters expressed on EC [8]. Active physiological or disease-induced drug targeting strategies use modified drugs to take advantage of native BBB nutrient transport systems or by conjugation to ligands that recognize receptors expressed at the BBB [37]. So, only drugs that closely mimic the endogenous carrier substrates will be transported into the brain. Nowadays, the research of nanoparticles to target BBB is in RMT, AMT and P-gp mechanisms, mainly [37].

Accordingly to AMT, the most limitation of this approach is lack of tissue selectivity, which can potentially cause side effects [38]. Its approach is based on SynB vectors, penetratin and Tat which are various examples of cell penetrating peptides [12]. Cell penetrating peptides have an enormous potential for diagnostic and therapeutic applications because their low cytotoxicity and the tremendous variety of cargo that can be loaded [8]. Recently, Liu and co-workers made a polymer core-shell NPs and on its surface is an anchored Tat molecule. The results shown that the surface with TAT improved their uptake cellular by EC [39].

RMT has been successful in transporting large drug molecules, drug carrying lipossomes, nanoparticles and polymeric complexes even without it [37]. As referred before, RMT has

different types of receptors and each receptor has its specific ligands and approaches [8]. In the case of diptheria receptor, it is strongly up-regulated in inflammatory conditions, which occur in CNS diseases. Recently, Boer and his group worked in CRM197 which is a non-toxic mutant of diphtheria toxin and applied it as a targeting vector for drug delivery to the brain in diagnostic and therapeutic applications [8].

At present, P-gp is considered the most prominent element of selective because it limits xenobiotics from entering and accumulates in the brain. So, one of the strategy is inhibits efflux transport systems by coating the nanoparticle surface with polaxamer 188 and polysorbate 80, for example. Polysorbate 80 is an important component because it is cleared adsorb apolyprotein E or B and followed by endocytosis and trancytosis.

## 3.2. Administration strategies

Regarding to direct delivery to CNS, there are different approaches. Accordingly to intracerebral (intraparenchymal) delivery, drugs are delivered directly into the parenchymal space of the brain. They can be injected by intrathecal catheters, by controlled release matrices and by microencapsulated chemicals or recombinant cells [3]. Unfortunately, access to the parenchyma is minimal so that a larger dose is required [8]. Alternatively, convection enhanced diffusion is used to increase drug uptake by bulk flow. Furthermore, brain implants (biodegradable/non-biodegradable polymeric materials encapsulating drugs) can be used for the local delivery, too [37]. Another possible route is the intraventricular route, which it is also used for drugs (small or large molecules) that do not cross the BBB and where no BBB drug delivery is available [40]. Lastly, the intrathecal route involves delivery of drugs into the cistern magna of the brain. In this delivery there is a chance of drugs spreading along the distal space of spinal canal. For this reason it is best used to treat spinal diseases [3].

Another possible to administer drug-loaded is the direct systemic delivery. In intravenous delivery, the most commonly used route to administrate larger doses of drugs into the body [41], the drug is deliver directly into the general circulation by avoiding its first-pass metabolism and has great potential to deliver drugs to almost all neurons in the brain. Unfortunately, drug availability is affected by its exposure to peripheral organs and rapid clearance. Consequently, there is only a little accumulation of the drug in the brain. Similarly, intra-arterial administration allows drugs to access the brain vasculature, before they enter peripheral tissue and it is possible to avoid first pass metabolism. By using BBB disrupting agents it is possible to increase the effects of this route [3]. The intranasal route is based on the principle that drugs exit the submucosa space of the nose into the brain CSF compartment. The nasal epithelium has many advantages such as high permeability, avoidance of first-pass metabolism, small doses and self-administration. However, this administration damages the nasal mucosa and decreases the quantity of drug available [23].

### 3.3. Chemical Stimuli

Parallel to last strategies, there has been a significant effort in delivering drugs to the brain with BBB disruption [63]. In this approach the substances are directly delivered to the CNS by using certain chemical substance or by applying energy (ultrasonic waves or electromagnetic radiations). However, the BBB disruption exposes the brain to infection and damage from toxins [6].

## 4. BBB models

It is, indisputable that *in vivo* models are the best candidates to study the permeability phenomena at BBB. However, these resources, typically rats or mice, are scarce, expensive, and difficult to study both in detail and real-time. Conversely, *ex vivo* and *in vitro* models are good alternatives due to their simplicity and controlled environment [11]. Nevertheless, the research community also recognizes that reproducing the physiology and the functional response of the BBB *in vitro* is a challenging task. *In vitro* BBB models started to emerge in early 1990s and offer a number of desirable advantages such as cost effectiveness, versatility enable controlled, repeatable and non-invasive tests like permeability assays, resistance measurements and microscopy. Moreover, they can alter multiple BBB determining factors namely: use different cell isolation procedures, cell culture conditions, configuration of cells on culture and the cell types (origin and species) [9, 17]; use different systems, such as static or dynamic. Nonetheless, in vivo validation is still required [9]. In the follow paragraphs, it will be discuss different factors and/or variables that can improve the BBB model and the different approaches that have been used to reproduce *in vivo* BBB.

### 4.1. Criteria for *in vitro* models of the BBB

At present no *in vitro* model can faithfully reproduce all the properties and characteristics of the *in vivo* BBB model since the latter has several types of cells and junctions that give rise to unique properties [7]. Considering that a single different factor is enough to change the BBB fundamental properties, there are several requirements that an ideal in vitro BBB model should meet. These include:

- The ability to enable the expression of TJ between adjacent EC which directly facilitate the formation of a selective barrier [9, 42];
- In vivo-like asymmetric distribution of relevant transporters which confers polarization of the EC [9];
- Mechanotransductive effects of shear stress from fluid flow on EC which determines cell differentiation and tight junction formation [42];

- The ability to discriminate the permeability of substances according to their molecular weight [9, 42];
- Maintenance of high electrical resistance that represents the maturity and soundness of the structures [43];
- The ability to reproduce the effects of a large variety of hemodynamic and systematic/inflammatory insults on the BBB [9];
- Availability, convenience, predictability and reproducibility [17].

An ideal BBB model should be able to reproduce all these characteristics. Unfortunately, the techniques available at present do not allow the monitoring of all these features. Therefore, new artificial systems such as bioreactors will have to incorporate a number of controlled parameters namely control/adjust oxygen and carbon dioxide levels in the culture medium, real-time monitoring of BBB integrity, medium sampling, among others. They will also have to include an array of computer-controlled sensors to monitor a variety of physiological parameters (e.g. glucose, lactate). Advances in this field will only be made possible with the introduction of new cell culture apparatus [9].

## 4.2. Overview of current *in vitro* BBB models

In the last decades we have witnessed the development of cell culture techniques in which cells are immersed in a homogeneous culture medium [44]. The main advantage of cell culture is that it allows us to select the stimuli that cells are exposed to, something that would be very difficult to reproduce *in vivo*. Besides, using different types of BBB cells, it will be possible use various apparatus which are possible to distinguish into two main groups: static and dynamic systems. The main difference is that dynamic models include fluid flow. However, most often the final choice of the BBB model is determined by the researcher's needs as well as the characteristics of the laboratory, namely time, cost and to what extent the model has to be able to reproduce in vivo conditions. Accordingly, either one or the other model can be more advantageous depending on the purpose of the investigation [43]. In the following sections current in vitro models of the BBB are analyzed; for improve understand of each model it will be referred to the corresponding key publications.

### 4.2.1. Cell types

Nowadays, most of the current successful BBB in vitro models are based on primary cell cultures [4] due to their high TEER values and low passage brain EC retain which closely resemble *in vivo* models, although the several passages of initial cultures entail the down-regulation or even the loss of many features [17]. Moreover, there may be a limitation in the availability of the primary cells as a result of the accessibility of the animals, while these cells are also more susceptible to internal and external contaminations than cell lines. In

addition, this approach has high costs and requires time-consuming and special skills for the isolation of brain EC. Primary cultures can use mammals such as rats, mice, pigs and bovines. Rodent models are advantageous in that they are available and it is possible to use them as transgenic animals [17]. However, their small size and the relatively low amounts of EC that can be obtained from them leads to the use of other models, namely pigs or bovines [45]. Not only it is possible to obtain large quantities of EC (up to 200 million as opposed to 1-2 million cells per rat brain) [7], but they also offer good permeability properties, more closely to the human BBB. On the other hand, their availability is restricted and they are not so well characterized regarding their biochemical or molecular composition [5]. Finally, the use of human primary cells is equally restricted by the unavailability of experimental material. The source material is usually acquired either from autopsies or biopsies, so this tissue often cannot be considered as a healthy resource [4]. Therefore, it was necessary to develop immortalized several cell lines [46].

Immortalized cell lines offer a considerable number of advantages. They are reliable (using trusted well-established sources), consistent (cell source is controlled and consistent), long-lasting (important cell features do not disappear over time), accessible (cells are available to be purchased at any time) and preparation time and cost are reduced [44]. Despite lacking certain BBB features and having low TEER, there is no doubt that immortalized cell lines are an emergent solution for BBB models. Immortalized cell lines are available from many species, although the most frequently used models derive from rats [47]. Other models of cell lines are the porcine and bovine ones. Though they are available, unfortunately they are far less well characterized. They have been used to study changes in protein expression following induction by astrocytes and neuroinflammatory responses [4]. Human cells became available in the early 1980s and contain excellent characteristics for the study of the developmental and pathophysiological processes of the BBB. The best characterized human cell line is the hCMEC/D3 which has been shown to retain important BBB characteristics. The hCMEC/D3 cells show a stable phenotype, the expression of endothelial cell markers, chemokine receptors and ABC-transporters. Furthermore, the paracellular permeability is much lower compared to other cell lines [48]. Human specimens are undoubtedly the best model, since they are the only ones that faithfully reproduce the BBB characteristics [4].

As previously mentioned, EC are the principal components of the BBB. However, in the course of time it was discovered that other cell types also play an important role both in the function and regulation of BBB characteristics. As a result, in vitro models became more complex as they began to include glial cells, pericytes, even neurons and microglia in different BBB models [7].

Co-culture of EC with glial cells increases TEER by 71 %. It is clear that these cells work in synergy to faithfully reproduce the BBB characteristics [44]. There is a formation of more stringent inter-endothelial TJ, which in turn constitute a more reliable reproduction of in vivo BBB [49].

With pericytes, it has been established that there is an intrinsic relation between pericytes and the formation and maintenance of the cerebral microvasculature structure and functions. However, it is still unknown which type of pericytes plays the decisive role in this process [43]. More recently, it has been proved that neurons induce BBB related enzymes in cultured EC. And the co-culture of these cells has shown that a direct contact among EC and neurons is not necessary for the induction of occludin expression [4].

**4.2.2. Apparatus**

The system semi-permeable plate filters, a vertical side-by-side diffusion support, is the most commonly used apparatus for EC culturing. This bidimensional model is a microporous semi-permeable membrane that separates the luminal (vascular) and the abluminal (parenchymal side) compartments and which is submerged in feeding medium [11]. This apparatus is ideal to study permeability of drugs across BBB. There are two other main features that make this apparatus so attractive: it is easy to establish cultures and its cost is relatively low [15]. On the other hand, the semi-permeable membranes cannot reproduce the physiological shear stress. In addition, the lack of antimitotic influences by laminin and flow will increase cell cycle rate, which will cause an uncontrolled growth of the EC in a multilayer manner. When the tightness of the semi-permeable barrier is measured by TEER and permeability it is usually much lower than the *in vivo* BBB [9]. The source of the cells and the methodology employed determine the kind of studies that may be performed: drug transposition through BBB, regulation of BBB permeability and influence of pathologies on BBB permeability [43].

Culturing cells using tri-dimensional extracellular matrix supports is another recently apparatus [50]. Among its main advantages we can list the capacity to enable close interactions between cells as well as the formation of quasi-physiological biochemical gradient exposure. Furthermore it is good to study specific roles of various extracellular proteins in cell differentiation. Despite these advantages, it is more expensive and less convenient than static models while, at the same time, it is a complex challenge to address. Nowadays, this type of model is applied to drug discovery and transport studies related to a variety of organs and tissues [51].

As opposed to static models, dynamic ones use physical stimuli to create shear stress and, as a result, they are able to replicate the physiological environment of in vivo BBB [9]. Bussolari and co-researchers made the first attempt to enable the endothelial exposure to flow in vitro

by using a purpose-built cone and plate viscometer [52]. This apparatus allowed them to expose cells to a quasi/uniform laminar or pulsatile shear stress. In this case, the level of shear stress was determined by the cone angle and the angular velocity. However, since the flow represented was turbulent it did not faithfully reproduce the flow experienced in vivo. This aspect constitutes a serious disadvantage because it is not possible to obtain reliable and significant results. Nonetheless, this apparatus was very important as it was the first step to produce dynamic models of the BBB [23].

Realizing the importance of shear stress as a vital component of any in vitro model, researchers decided to focus on the development of new generations of dynamic in vitro systems of which a detailed explanation will follow. The main features of the dynamic *In vitro* Blood-Brain Barrier (DIV-BBB) are the possibility to use co-cultures and the presence of intraluminal flow through artificial capillary-like structural supports (hollow fibers) [15]. As a result, it is possible to faithfully reproduce the BBB in situ as the EC are cultured in the lumen of hollow-fibers inside a sealed chamber and are exposed to flow while the astrocytes are seeded in the extraluminal compartment to promote cellular stimuli. This system presents low permeability to intraluminal potassium and polar molecules, high TEER, negligible extravasation of proteins, the expression of specialized transporters, ion channels, and efflux systems. However, this system is not intended to be used in drug permeability studies and requires more time and technical skills to be established. Though it is possible to characterize cells, this can only be done in a limited way. Finally, to start the process a high cell load is required [9].

Recently the development of microtechnologies has enabled the creation of a new in vitro model of the BBB called MicroBBB. MicroBBB is a poly(dimethylsiloxane) multi-layered device with a membrane in between which separates the top and bottom channel. Although this apparatus is an entirely new creation, it also enables cell culturing procedure, permeability tests and TEER measurements [53]. When compared to the models previously discussed, MicroBBB presents more advantages including rapid and low-cost fabrication, controlled and repeated environment with realistic microcirculatory dimensions and environment, physiological fluid flow and shear stress and much thinner culture membrane which decreases the distance between co-cultured cells. However, the top-bottom architecture of this model limits simultaneous real-time visualization of both the vascular and neuronal sides of the BBB [4]. Another key feature of this model is that it can be used to monitor drug permeability, as well as changes in barrier function, which occur in response to various environmental stimuli namely diseases.

### 4.2.3. *In silico* models

The incredible development of computer technology and sophisticated algorithms allowed the creation of new methods based on computer simulation called *in silico* models [7]. *In silico* models offer various advantages, the most important of which lies in accurate predictions. Not only is there no need to recur to laboratory experiments, but the process is also cheaper and requires fewer time-consuming laboratory experiments [23]. The potential to accelerate drug discovery is the outstanding quality of *in silico* models for medicine. This technology allows the compounds to be synthesized, pre-screened, and virtually tested, so that it is possible to predict how they will cross the BBB. Therefore, it will be possible to study the efficacy and the bio-availability of novel drugs in terms of brain permeability, transport properties and toxicity [9]. On the other hand, the complex nature of BBB is not taken into full consideration, which leads to uncertain results. Though *in silico* models represent future breakthroughs in the pharmaceutical drug development, clinical studies will still have to be supported by *in vitro* and *in vivo* models in order to collect a number of crucial physicochemical measurements [7, 9] .

# Chapter 2

# Aim

The main goal of the present thesis was a further characterization and improvement of an *in vitro* BBB model, using three different type of human cells, as a tool to study biological and functional BBB alterations and as a key to assess permeability of anti-cancer drugs.

**General goals**

1. Develop an *in vitro* BBB model that will mimic more properties and characteristics of the *in vivo* BBB;

2. Integrity evaluation based on the alterations applied through the *in vitro* model;

3. Development of Camptothecin-loaded SLN (CPT-SLN) for brain delivery;

The thesis work was divided into two phases. First, it was analyzed the state of the art, definition of the work plan and requisition of the laboratory material. This part was done during September and October and also a few months before, during the 2$^{nd}$ semester. On the second phase was developed the laboratory work at Laboratory of Pharmaceutical Tecnnologic, Department of Drug Sciences, Pharmacy Faculty, University of Porto, the majority of the work, and at INEB, University of Porto. This part was realized from October until June.

To develop and evaluate the integrity of triple co-cultured model, it was seeded hCMEC/D3 cell line, primary human astrocytes and U87 cell line. During the time on culture, TEER measurements were taken. Moreover, on the last day on culture were performed different experiments such as permeability assay, immunocytochemistry, optical microscopy, electronic microscopy and flow cytometry to analyze the cell morphology, expression of cellular specific markers and barrier integrity.

Then, to develop CPT-SLN for brain delivery it was selected the drug-SLN formulation. And it was produced and characterized CPT-SLN by mean size, size polidispersity, surface charge and association efficiency. Finally, it was done viability assays using different CPT formulations.

# Chapter 3

# Materials & Methods

## Materials

Dulbecco's Modified Eagle's Medium (DMEM), Fetal Bovine Serum (FBS), glutamine, penicillin-streptomycin, chemically defined lipid concentrate, HEPES and trypsin-EthyleneDiamineTetraacetic Acid (EDTA), Occludin-mouse monoclonal antibody-Alexa Fluor 594, Claudin-5-mouse monoclonal antibody-Alexa Fluor 488, N2 suplemment, Wheat Germ Agglutinin (WGA) – Alexa Fluor 488 and Geltrex™ LDEV-Free Reduced Growth Factor Basement Membrane Matrix were provided by Gibco (Invitrogen Corporation, Spain). Hidrocortisona - γ-irradiated, Dulbecco's Phosphate Buffered Saline (DPBS) Modified, without calcium chloride and magnesium chloride, fluoroshield™ with 4',6-diamidino-2-phenylindole, dihydrochloride (DAPI) mounting medium, paraformaldehyde, giemsa stain, rat tail collagen type I, human basic fibroblast growth factor (bFGF), ascorbic acid, lithium chloride solution, Fluorescein isothiocyanate – Dextran (FD) average molecular weight of 4.000, 40.000 and 70,000 Da, triton-X 100, Bovine Serum Albumin (BSA) were provided by Sigma-Aldrich (Portugal). EBM-2 medium were provided by Lonza. The 12-well semi-permeable plate filters, PE-mouse anti-human GFAP were sold by BD, Biosciences, USA. VE-Cadherin-FITC were obtained from Miltenyi Biotec (USA). AlamarBlue™ cell viability reagent assay were obtained by Thermo Scientific (USA).

Cetyl palmitate was a gift from Gattefossé SA, (St Priest, France). The surfactant polysorbate 80, organic solvents (acetonitrile, triethylamine) for high performance liquid chromatography (HPLC) and Dimethyl sulfoxide (DMSO) were supplied by Merck KgaA, (Darmstadt, Germany). Purified water was of MilliQ ® -quality.

# Methods

## 3.1. Cell Culture

### 3.1.1 - Cells description

Immortalized mouse EC (b.End3) cell line is sold by American Type Culture Collection. bEnd3 is an immortalized mouse EC. The cells were transformed by infection with the NTKmT retrovirus vector that expresses polyomavirus middle T antigen. The endothelial nature of these cells was confirmed by the observed expression of von Willebrand factor and uptake of fluorescently labeled low density lipoprotein (LDL).

Immortalized human brain capillary EC (hCMEC/D3 cell line) was a kindly donated by Dr. PO Couraud (INSERM, France). The original brain EC used for the generation of the cell line were isolated from human brain tissue following surgical excision of an area from the temporal lobe of an adult female with epilepsy. The hCMEC/D3 cell line had been immortalized by lentiviral transduction of the catalytic subunit of human telomerase and SV40-T antigen into very early cultures of adult human brain endothelial microvascular cells [54]. hCMEC/D3 between passage 25 and 33 were used in all studies.

The human astrocytoma U87 cell line is a commercial cell line sold by American Type Culture Collection. It derived from a human glioblastoma (astrocytoma), classified as grade IV as of 2007 with adherent properties.

Primary astrocytes are human brain progenitor-derived astrocytes with adherent properties sold by Gibco. It is the only that are primary cells, so the number of cells is more limited than the other ones to perform the *in vitro* models experiences.

#### 3.1.1.1 Cell line conditions

For culturing, hCMEC/D3 were seeded in a concentration of 25 000 cells/$cm^2$ and grown in EBM-2 medium (Lonza, Basel, Switzerland) supplemented with 10 mM HEPES, 1 ng/mL human Basic Fibrolast Growth Factor (bFGF), 1.4 µM hydrocortisone, 5 µg/mL ascorbic acid, penicillin–streptomycin, chemically defined lipid concentrate and FBS. All culture ware and semi permeable filters were coated with 150 µg/mL rat tail collagen type I for 1 h at 37° C. Collagen is a fibrous protein which presents a rope-like triple helix, providing strength to the extracellular matrix and this specific type of collagen is the most common fibrillar collagen (90%). Cells were cultured in the incubator at 37° C with 5% $CO_2$, 95% fresh air in a humidified incubator (Heraeus Hera Cell incubator). Cell culture medium was changed every 2-3 days.

The human glioma U87 cell line and b.End3 cell line were maintained in complete Dulbecco's Modified Eagle's Medium (DMEM) (Gibco, Invitrogen Corporation) supplemented with 10% fetal

bovine serum (FBS), 1% glutamine (2mM) and 1% antibiotic-antimycotic (Gibco, Invitrogen Corporation: 10,000 units/mL penicillin G sodium, 10,000 mg/mL streptomycin sulphate). Cells were subcultured every 3-4 days using trypsin-EDTA.

Primary astrocytes were maintained in complete Dulbecco's Modified Eagle's Medium (DMEM, Gibco, Invitrogen Corporation) supplemented with 10% fetal bovine serum (FBS), 1% glutamine (2mM), 1% antibiotic-antimycotic (Gibco, Invitrogen Corporation: 10,000 units/mL penicillin G sodium, 10,000 mg/mL streptomycin sulphate) and 1% N2 supplemment (Gibco, Invitrogen Corporation). The medium has been specifically formulated for the growth and maintenance of human astrocytes while retaining their phenotype. All culture ware and semi permeable filters were coated with 0.1 mg/mL Geltrex™ LDEV-Free Reduced Growth Factor Basement Membrane Matrix (Gibco, Invitrogen Corporation) for 1 h at 37° C. It is used for promotion and maintenance of many cell types specifically primary cells. The major components of this matrix product include laminin, collagen IV, entactin and heparin sufate proteoglycan. Cells were subcultured every two times per week using trypsin-EDTA.

## 3.1.2 - Cell line laboratory concepts

### 3.1.2.1 - Cell subculture

Firstly, the cells were examined to inverted microscopy to study any signal of contamination. When the cells present 70-80% of confluence, the medium was aspirated and they were washed with Dulbecco´s Phosphate Buffered Saline (DPBS) two-three times to remove all residues. Then, they were detached using trypsin-EDTA (1x) from the flask, only a few minutes because trypsin cuts the adhesion proteins in cell-cell and cell-matrix interactions and EDTA is a calcium chelatator, so it is necessary to pay attention of the time in contact with the cells. In this way, it was necessary added medium to block the action of this enzyme. The cell suspension was put in a tube and centrifuged at 1500 rpm, 21 ºC during 5 minutes. After the centrifuge, it was removed the supernatant and the pellet was mixed and resuspend in medium. To count the cells, it was necessary to pipette 10 µL of cells and 90 µL of trypan blue and it was expelled the cell suspension immediately to the edge of the Neubauer chamber. Then, under the inverted microscope the viable cells were counted. Using the following formula it was possible to know the number of cells in total volume (where n=number of cells in Neubauer chamber; d=dilution ratio).

$$\frac{n}{4} \; x \; \frac{1}{d^{-1}} \; x \; 10^4 = number\ of\ cells/mL$$

#### 3.1.2.2 - Cell freezing

Instead of using the cells for subculture, it is better freeze them, in order to prevent phenotypic degeneration, characteristic of high passage numbers. For that, following the method before, after counted the cells the pellet was gently resuspended in Freezing medium consisting of complete culture medium with 5-10% (v/v) DMSO (Sigma), a cryopreservant, and transferred to adequate cryovials, on concentration of 2-3 millions of cells per 2 mL. These cryovials were stored at -80ºC freezer.

#### 3.1.2.3 - Cell thawing

To prevent prevent as faster as possible the DMSO of the freezing medium, a cryovial was rapidly removed and thawed in a 37ºC water bath. Cells were transferred to complete medium and centrifuged at 1500 rpm for 5 minutes. The supernatant were discarded and the pellet was gently ressuspended in pre-warmed complete medium and transferred to tissue culture flasks.

## 3.2 *In vitro* models

Firstly, to improve laboratory skills and to learn how to manipulate an *in vitro* model it was performed monocultures using bEnd3 cell line on the semi-permeable filters. Then, monocultures of hCMEC/D3, co-cultures of hCMEC/D3 and U87 cell line, co-cultures of hCMEC/D3 and primary astrocytes and a triple co-culture of hCMEC/D3, U87 cell line and primary astrocytes cells were cultured on semi-permeable plate filters which was developed based on a rather simplified view of the BBB, Figure 3.1. The semi-permeable filter is composed by an insert filter and an acceptor well, with the apical chamber mimicking the blood and the basolateral one mimicking the brain side.

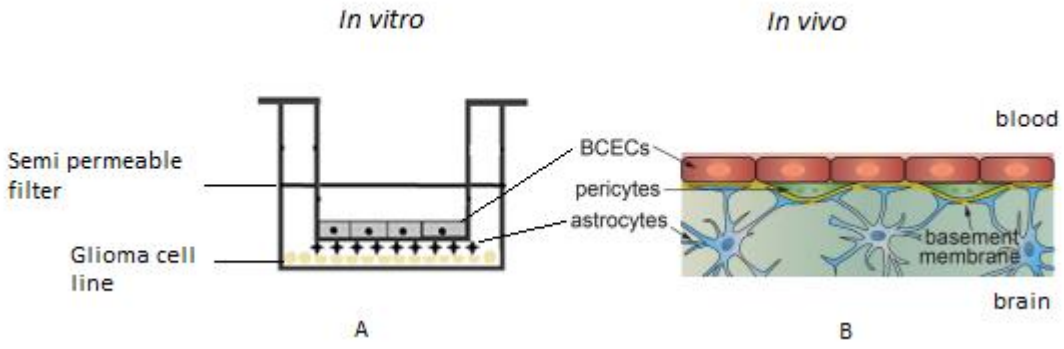


**Figure 3.1** Schematic illustration of [A] *in vitro* BBB model and [B] *in vivo* BBB. Endothelial cells will seeded on the apical chamber (blood) which is in the internal part of the *in vitro* model. Astrocytes will seeded on the inverted side of the insert in basolateral chamber (brain) but in direct contact with endothelial cells and the glioma cell line will seeded also on the basolateral chamber (brain), however in the bottom of the plate. Adapted from [55].

The microporous membrane interface allows nutrient exchange and the passage of cell-derived and exogenous substances. The specific model selected for this work was the 12-well clear polyester semi-permeable plate filters, which features a vertical side-by-side diffusion system with 1.0 µm pore size. It has tissue-cultured treated surface; effective growth area of membrane about 0.9 $cm^2$ and membrane diameter about 10.5 mm. The properties of the clear membrane allow an easier observation under the microscope. Furthermore, the smaller size membranes are primarily used in drug transport studies and it is suitable for the study of co-cultures as cell migration.

The apical part of the insert was filled with 0.5 mL and the basolateral side with 1.5 mL. To avoid to the monolayer uneven hydrostatic pressure, it was aspirate medium from the bottom first. When adding fresh medium, it was filled the top chamber first. For the same reason, it is important to consider the amount of media in each chamber, so the height of the fluid in the chamber should be at same level as inside.

## 3.2.1 *In vitro* models development

### 3.2.1.1 Endothelial rat cells on monoculture

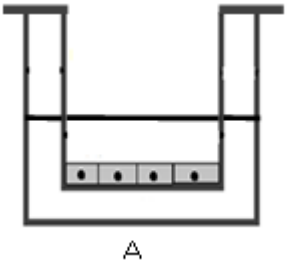


**Figure 3.2** The experimental procedure for monoculturing the bEnd3 cell line. [A] Endothelial cells were seeded onto the luminal side of the semi-permeable filter during 7 days.

Endothelial mouse cells were seeded at initial concentration of $1.8x10^5$ cells/$cm^2$ and of $0.9x10^5$cells/$cm^2$, Figure 3.2. Cells were cultured during 21 days in the incubator at $37^0$ C with 5% $CO_2$, 95% fresh air in a humidified incubator (Heraeus Hera Cell incubator). Cell culture medium was changed at 3 days.

During the time on culture, the resistance of the barrier was analyzed.

### 3.2.1.2 - Endothelial human cells on monoculture

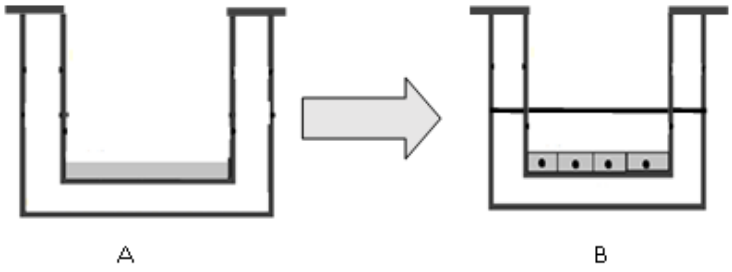


**Figure 3.3** The experimental procedure for monoculturing the endothelial cells. [A] The filter was coated with rat tail collagen type I during 1 hour and [B] Endothelial cells were seeded onto the luminal side of the semi-permeable filter during 7 days.

Before seed the cells, it was necessary to coat the membrane with rat tail collagen type I (Invitrogen, Gibco) at 150 ug/mL during 1 hour, Figure 3.3 – A. Then, it was washed the filter with DPBS because of the acetic acid present on this collagen solution. hCMEC/D3 cell line was cultured, Figure 3.3 – B, at different concentrations at $5x10^4$ cells/$cm^2$; $4,6x10^4$ cells/$cm^2$; $2,3x10^4$ cells/$cm^2$ and $1,15x10^4$ cells/$cm^2$ on the apical side of the semi-permeable filter. Cells were cultured during 11 days in the incubator at 37º C with 5% $CO_2$, 95% fresh air in a humidified incubator (Heraeus Hera Cell incubator). In the follow experiments was used the $4,6x10^4$ cells/$cm^2$ initial concentration during seven days on cell culture. Cell culture medium was changed at $2^{nd}$, $4^{th}$ and $7^{th}$ days and it was added lithium chloride with fresh medium.

During the time on culture, the resistance of the barrier was analyzed. Also, to characterize the model it was performed permeability assays, flow cytometry analysis, immunocytochemistry technique and optical microscopy using giemsa.

### 3.2.1.3 –EC and U87 cell line on co-culture

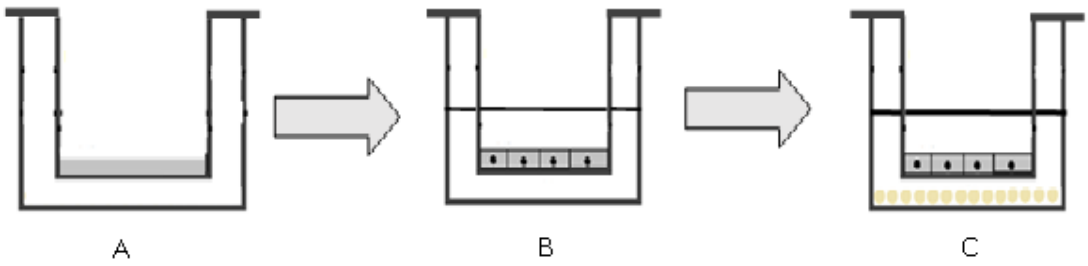


**Figure 3.4** The experimental procedure for co-culturing the endothelial cells and U87 cell line. [A] The filter was coated with rat tail collagen type I during 1 hour. Then, [B] Endothelial cells were seeded onto the luminal side of the semi-permeable filter and [C] On $2^{nd}$ day, U87 cell line was seeded on the abluminal side of the model with the same initial concentration of endothelial cells and co-cultured for 5 days.

Initial was used the same procedure to culture endothelial human cells, Figure 3.3 - A and B. At the end of the second day was added U87 cell line in the same initial concentration of EC,

$4{,}6x10^4$ cells/$cm^2$ at the abluminal side, Figure 3.4 - C. Cells were cocultured for an additional 5 days in the incubator at 37º C with 5% $CO_2$, 95% fresh air in a humidified incubator (Heraeus Hera Cell incubator). Cell culture medium was changed at 2nd, 4th and 7th days and it was added lithium chloride with fresh endothelial medium on the luminal side and DMEM complete on the abluminal side of the *in vitro* model.

During the time on culture, the resistance of the barrier was analyzed. Also, to characterize the model it was performed permeability assay, flow cytometry analysis, immunocytochemistry and Scanning Electron Microscopy (SEM).

**3.2.1.4** – EC **and astrocytes on coculture**

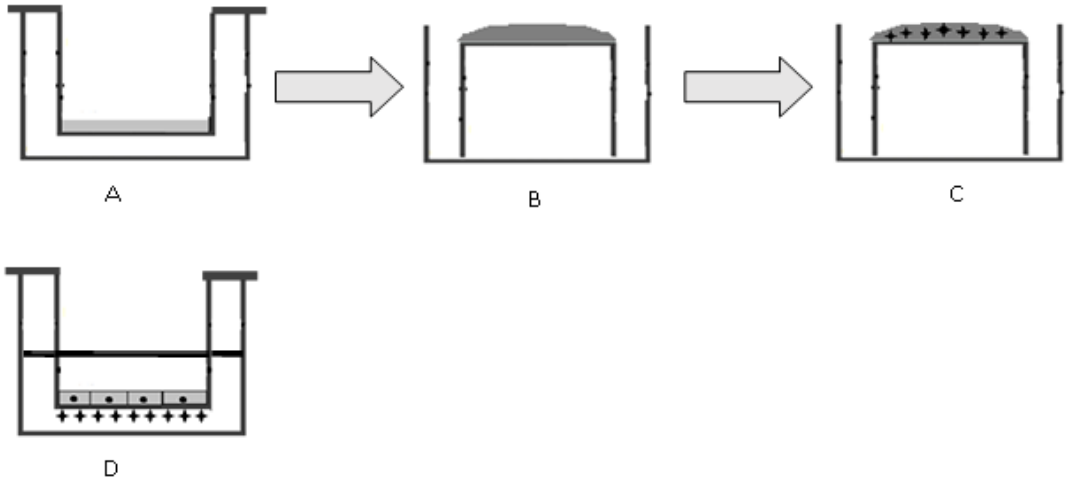


**Figure 3.5** The experimental procedure for coculturing the endothelial cells and astrocytes on different sides of the semi permeable filter. [A] The filter was coated with rat tail collagen type I during 1 hour. Then, [B] the filter were coated with Geltrex, basement membrane substitute. [C] Astrocytes were first seeded onto the abluminal side of the inverted semi permeable filter and allowed to adhere for 3h. [D] The filter was flipped back and endothelial cells were seeded onto the luminal side of semi-permeable filter and cocultured with astrocytes for 7 days.

Before seed the cells, it was necessary coated the membrane with rat tail collagen type I, Figure 3.5 - A. Then, it was added Geltrex (Invitrogen, Gibco) to coat the other side of the insert during 1 hour, Figure 3.5 – B. The main goal of this coating is to permit the fast differentiation and growth of the primary astrocytes. Then, it was culture astrocytes at ratio 1 to 23 EC in the opposite side of the insert and are maintained in this position during 3 hours, when necessary medium was added, Figure 3.5 - C. The filter was flipped back and it was seeded EC on the abluminal side, Figure 3.5 - D. Cells were cocultured during 7 days in the incubator at 37º C with 5% $CO_2$, 95% fresh air in a humidified incubator (Heraeus Hera Cell incubator). Cell culture medium was changed at 2nd, 4th and 7th days and it was added lithium chloride with fresh endothelial medium on the luminal side and DMEM complete with N2 supplemented on the abluminal side of the *in vitro* model.

During the time on culture, the resistance of the barrier was analyzed. Also, to characterize the model it was performed permeability assay and Scanning Electron Microscopy (SEM).

**3.2.1.5 – EC, astrocytes and U87 cell line on cell culture**

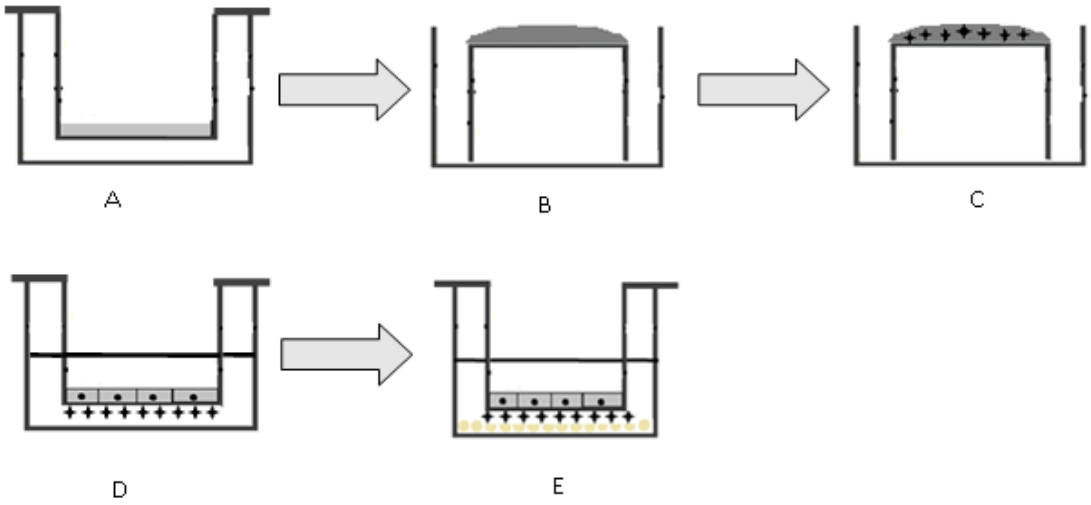


**Figure 3.6** The experimental procedure for co-culturing the endothelial cells, astrocytes and U87 cell line on different sides of the semi permeable filter. [A] The filter was coated with rat tail collagen type I during 1 hour. Then, [B] the filter were coated with Geltrex, basement membrane substitute. [C] Astrocytes were first seeded onto the abluminal side of the inverted semi permeable filter and allowed to adhere for 3h. [D] The filter was flipped back and endothelial cells were seeded onto the luminal side of semi-permeable filter and co-cultured with astrocytes for 7 days. [E] On 2nd day, U87 cell line was seeded on the abluminal side of the model with the same initial concentration of endothelial cells and cultured for an additional 5 days.

Initial was used the same procedure to co-culture EC and astrocytes, Figure 3.5 - A and D. And, at second day was added U87 cell line at same initial proportion of EC, Figure 3.6 - E. Cells were co-cultured for an additional 5 days in the incubator at 37º C with 5% $CO_2$, 95% fresh air in a humidified incubator (Heraeus Hera Cell incubator). Cell culture medium was changed at 2nd, 4th and 7th days and it was added lithium chloride with fresh endothelial medium on the luminal side and DMEM complete with N2 supplemented on the abluminal side of the *in vitro* model.

During the time on culture, the resistance of the barrier was analyzed. Also, to characterize the model it was performed permeability assay and Scanning Electron Microscopy (SEM).

## 3.2.2 - In vitro models characterization

**3.2.2.1 – TEER**

In order to be sure the amount and formation of endothelial tight junctions, the cell monolayer integrity was periodically inspected under a microscope and TEER were performed using an EVOM voltohmmeter (World Precision Instruments, Sarasota, FL, USA). Briefly, the lengths of the electrodes are unequal allowing the longer electrode (external) to touch the

bottom of the basolateral side while preventing the shorter electrode (internal) from reaching the bottom of the apical side. An increase of TEER values indicate an increase of the confluence of the monolayer and of its integrity. The resistance value ($\Omega \times cm^2$) of an empty filter was subtracted from each measurement. Six measurements were taken per filter, and each culture condition was performed with triplicate filters to obtain average TEER and standard deviation.

#### 3.2.2.2 Permeability transport experiment

The apparent permeability based on the flux of a molecule across the barrier with known molecular weight can be also a measure of the integrity of the *in vitro* BBB model. The fluid flux is linearly proportional to the dose applied. So, more abluminal fluorescence units more it will be the molecule quantity that had crossed the barrier.

On 7$^{th}$ day, the integrity of the membrane was accessed by FD4 (average molecular weight 4.000 Da), FD40 (average molecular weight 40.000 Da) and FD70 (average molecular weight 70.000 Da) permeabiliites at initial concentration of 1 mg/mL. Each solution of FD was dissolved on EBM-2 and it was added 500 µl to the upper chamber of the semipermeable plate filters and on the bottom chamber, it was added only DMEM. The plate was homogenized during 1 minute, before sampled. The lower chamber was sampled at various time periods (30, 60, 90, 120 and 150 minutes), and the amount was determined using a fluorescence multiwall plate reader at excitation wavelength to 488 nm and the emission wavelength to 520nm.

The apparent permeability (Papp) was calculated using the following equation:

$$Papp = \frac{Q}{AxCxt}$$

Where Papp is the apparent permeability (cm/s), Q is the amount of molecule transported per minute (µg/min), A is the surface area of the filter ($cm^2$), C is the initial concentration of the molecule and t is the time (seconds). The data it will be presented graphically as a percent change from control values.

#### 3.2.2.3 Flow cytometer studies

To confirm the initial seeding proportions and guarantee the glioma cell line and endothelial phenotype, flow cytometry experiments were done using specific astrocyte and endothelial markers. On preliminary studies, it was tested different incubation times, temperatures and antibody ratio. Control negative experiments were done in parallel.

Cell suspensions of hCMC/D3 cells were prepared from confluent cell monolayers dispersed with trypsin-EDTA. The VE-Cadherin marker plays a fundamental role in maintaining endothelial integrity, barrier function, and leukocyte extravasation. Loss of VE-cadherin expression from/or disorganized VE-cadherin distribution at cell junctions directly influences monolayer integrity and endothelial permeability. After obtained a cellular suspension, cells were centrifuged at 300xg for 10 minutes. Upon washing with DPBS containing 0.5 % BSA and 2mM EDTA buffer, the cell pellet was resuspended in 100 µL DPBS containing 0.5 % BSA and 2mM EDTA buffer with 10 µL of the VE-Cadherin- FITC antibody and incubated at 4-8 ºC during 30 min.

Upon washing and centrifuged, the cell pellet of all samples were resuspended on 100 µl of DPBS and were performed flow cytometry analysis using BDFACS Calibur (BD Biosciences, USA).

Briefly, the solution of 0.5 % BSA and 2mM EDTA buffer is used, because EDTA can avoid cell clumps during flow cytometer acquisition and BSA compound reduces the chance of heterophilic antibody interference and can decrease non-specific binding of the antibodies.

**3.2.2.4 - Immunofluorescence**

Membrane markers

On the 2$^{nd}$, 4$^{th}$, 7$^{th}$, 9$^{th}$ and 11$^{th}$ days, cells were washed three times with DPBS and fixed in 4% paraformaldehyde for 10 min. The cell membranes were labeled with 5.0 µg/mL Alexa Fluor 488–WGA, incubated for 10 minutes at 37°C. After three washes with DPBS, the cells nuclei were labeled 4′, 6-Diamidino-2-pheny-lindoldihydrochloride (DAPI) at a concentration of 300 nM for 5 min at 37°C. Cells were washed an additional three times in PBS and visualized using a Nikon Eclipse E4000 (Nikon Instruments Inc., USA). Photographs were run by NIS Elements (Nikon Instruments Inc., USA).

Endothelial specific markers

On the 7$^{th}$ day, the cells were washed three times with DPBS and fixed in 4% paraformaldehyde for 10 min at room temperature (RT). They were then washed three times for 5 minutes with DPBS. Upon washing, cells were permeabilized by incubating for 10 minutes with 0.1% (v/v) Triton X-100 in DPBS. Following permeabilization, cells were washed for 5 minutes with DPBS. In order to prevent non-specific binding, it was added a blocking solution DPBS with 0.05% Tween 20 containing 3% (w/v) BSA for 30 minutes. Then the antibody was dilute to its optimal working concentration in appropriate dilution DPBS containing 0.5 % BSA and 2mM EDTA at ratio 1:100 (Claudin-5-Alexa Fluor 488, Occludin-Alexa Fluor 594) and at ration 1:10 VE-Cadherin-FITC. In case of VE-Cadherin marker, it was not

submitted to the permeabilization procedure. It was added 250 µL of diluted antibody per well and incubated during 30 minutes at 4-8 ºC. After three washes with DPBS, the insert membrane was removed and put onto the glass coverslips. Then, the cells nuclei were labeled with DAPI using the mounting medium and visualized using a Nikon Eclipse E4000 (Nikon Instruments Inc., USA). Photographs were run by NIS Elements (Nikon Instruments Inc., USA).

#### 3.2.2.5 - Giemsa staining

On the 2nd, 4th, 7th, 9th and 11th days, cells were fixed in methanol for 2 min and stayed on air dry at room temperature. The cell were labeled with Giemsa stain (1:20) during 30 minutes. Cells were washed several times with deionized water and visualized using an inverted microscope (Motic Incorporation). Briefly, giemsa stain is used to differentiate nuclear and/or cytoplasmic morphology, the nuclei will be varying shades of purple and cytoplasmic staining will be varying shades of light pink of the bone marrow cells.

#### 3.2.2.6 - Scanning Electron Microscopy

The surface of the EC and the astrocytes cells were observed by SEM on 7th day. Briefly, the insert membrane was removed and fixed with 3% glutaraldehyde in 0.1M sodium cacodylate solution solution pH 7.4 for 45 min at 4°C. Then, the membrane was washed with cacodylate buffer for 5 min. After dehydrated in graded ethanol, on the insert membrane was added HDMS solution for 10 minutes and air-dry. Finally, the samples were put on the support and coated with Au/Pd for 60 seconds and with a 15mA current. The samples were examined by a Quanta 400FEG ESEM / EDAX Genesis X4M.

## 3.3 Camptothecin loaded Solid Lipid Nanoparticles

SLN have a solid incomplete matrix. These nanoparticles have a hydrophobic core, an ideal solution to transport hydrophobic drugs, avoiding drug degradation for example. As a result, the strategy is incorporate an anti-cancer drug, camptothecin, as target U87 cell line and cross the BBB, into SLN. In the sequence of the work done by Martins and co-researchers [35, 56, 57] in the production and characterization of this new drug model.

### 3.3.1 – Production of Solid Lipid Nanoparticles

#### 3.3.1.1 - High shear homogenisation followed by ultrasonication

For smaller particle size combination of both ultrasonication and high shear homogenisation is required. The formulations containing the lipid cetyl palmitate and the surfactants

polysorbate 80 were prepared at concentrations of 5% (w/w) of lipid, 2% (w/w) of surfactant and 0.01 % (w/w) of camptothecin. The lipid and surfactant mixture was melted at approximately 5 to 10 ºC above the melting point of the lipid. This mixture is then combined with an aqueous solution heated at the same temperature. A hot pre-emulsion is formed by high shear homogenisation using with an ultra-turrax T25 at 8000 rpm during 40 seconds. This hot pre-emulsion is converted into a nanoemulsion when processed in an ultrasonic probe at 80% amplitude for 2.5 min. The particle size is decreased mainly by cavitation. The nanoemulsion is cooled down leading to recrystallisation of the lipid and formation of lipid nanoparticles.

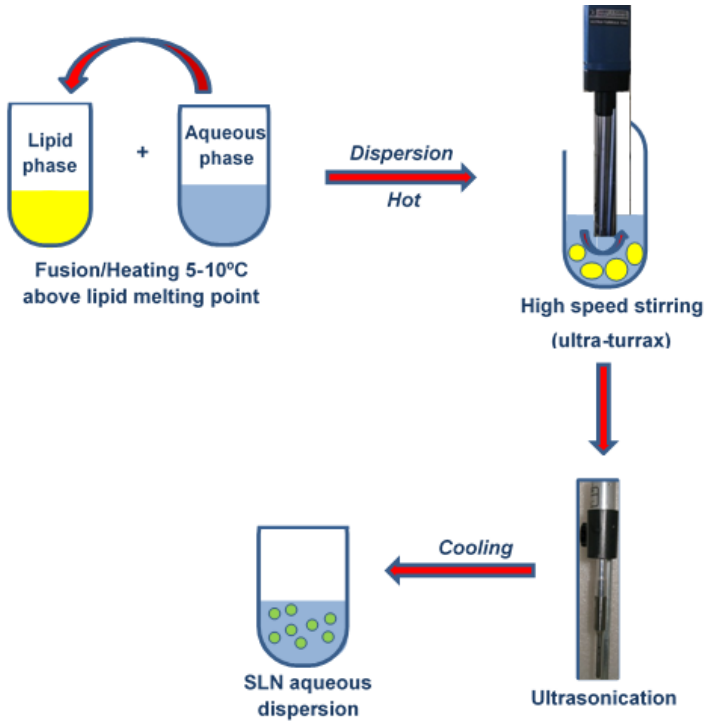


**Figure 3.7** Schematic representation of SLN production by high shear homogenisation followed by ultrasonication adapted from [35].

## 3.3.2 – Characterization

### 3.3.2.1 – Mean particle size and size distribution

To analyse the particle size and distribution of the nanoparticles were used two different equipments, Zetasizer Nano ZS laser scattering device and Malvern Mastersizer 3000.

Firstly, particle size and distribution (polydispersity index) was determined by dynamic light scattering (DLS), using a Zetasizer Nano ZS laser scattering device (Malvern Instruments Ltd., Malvern, UK) with a range from 0.0003µm to 10µm. Prior to the measurements, all samples were diluted (1:10) using purified water to yield a suitable scattering intensity, the average count rate indicates that the dilution applied to the formulations was appropriate. The

measurements were always performed in triplicate. The available software (Zetasizer Nano Series V6.20) was used to correlate the intensity of scattered light with the hydrodynamic radius of the spherical particle.

Briefly, DLS measures the light scattered from a laser that passes through a colloidal solution. As a result of the brownian motions, there are changes in scattered light intensity. So, DLS does not directly measure the diameter of particles, but rather detects the fluctuations of light signals caused by the Brownian motion of the particles to calculate their sizes. More DLS technique can give information about polidispersion index that indicates the state of particle aggregation of nanoparticles in suspension.

Laser diffractometry was additionally performed in order to analyse the particle size, using a laser diffraction particle size analyser (Malvern Mastersizer 3000, Malvern Instrument, Ltd) with a range from 0.01 to 3500 μm. The determination was performed at room temperature using 1.1 for the refractive index, 0.01 for the absorption index, laser obscuration around 6% and Scattering Model Mie. The dispersant was water with refractive index of 1,330. The particle size distributions of the nanoparticles were determined and the results were respectively expressed by the mean volume diameter (D [4, 3]), 10% percentile (D [0, 10]), median (D [0, 50]) and 90% percentile (D [0, 90]). The LD data were expressed using volume distributions, and given as diameter values corresponding to percentiles of 10%, 50%, and 90%. The span value is a statistical parameter useful to characterize the particle size distribution, and was calculated according to:

$$Span = \frac{(d90\% - d10\%)}{d50\%}$$

**3.3.2.2 – Surface charge**

The electrophoretic mobility (zeta potential) of the nanoparticles and ultimately their surface charge was measured by combining laser Doppler velocimetry and phase analysis light scattering (PALS) using a Zetasizer Nano ZS (Malvern, Worcestershire, UK). Surface charged particles within the dispersion migrated toward the electrode of opposite charge and the velocity of particles migration was converted in zeta potential values by using the Smoluchowski's equation. Zeta potential is a physical property present in any particle in dispersion and it is an indirect measurement of the surface charge. The magnitude of the zeta potential gives an indication of the potential long-term stability of the colloidal dispersions and also predict interactions between the nanoparticles and the cellular membranes that can occur due to electrostatic interactions.

### 3.3.2.3 – Association Efficiency

Association Efficiency were determined by two methods, indirect and direct one. In both methods camptothecin association efficiency was determined by High Performance Liquid Chromatography (HPLC), as previously described [56]. Briefly, the chromatographic analysis was performed at 30 °C on an analytical reversed-phase (RP) Mediterranea™ Sea18 column (150 mm × 4.0 mm, 5 µm, Teknokroma, Spain) protected with a precolumn Ultraguard™ (Guard column Sea18, 10 mm × 3.2 mm, Teknokroma, Spain). The optimised method used a binary gradient mobile phase with 1% (v/v) triethylamine buffer at pH 5.5 (pH adjusted with acetic acid) as mobile phase A and acetonitrile as mobile phase B. A flow rate of 1.2 mL/min was used with a 10 µL injection volume. The program started with a gradient of 75%A and 25%B and after 1 min the gradient changed continuously until the minute seven were it reaches the gradient of 40%A and 60%B which was maintained until minute nine. Afterwards, the gradient was changed again to 75%A and 25%B and remained constant until minute sixteen. The eluted peaks were monitored at excitation and emission wavelengths of 360 and 440 nm, respectively. Stock solutions of CPT were prepared daily in DMSO at concentration of 1 mg/mL and further diluted in 9 mM phosphate buffer pH3 to a concentration of 10 µg/mL. Standard solutions were prepared by dilution in 9 mM phosphate buffer pH3 o a final CPT concentration between 10 and 100 ng/mL.

Subsequently, the quantification of the compound was carried out by measuring the peaks areas in relation to the standards.

**Indirect Method**

Upon separation of camptothecin-loaded SLN from free camptothecin by ultracentrifugation. Prior to first ultracentrifugation (100,000×g, 20 min) SLN dispersions were diluted 10 times in PBS buffer 50 mM pH 10.5. The supernatant collected was further diluted 100 times in PBS buffer. And, the supernatant resulted from the second ultracentrifugation (100,000×g, 20 min) was analysed and the camptothecin concentration in SLN was detected indirectly by HPLC.

Using the indirect method, the association efficiency of a drug in SLN, the aqueous phase is separated from the lipid particles and subsequently drug content of the aqueous phase is determined. The amount of drug measured in the aqueous phase is considered the amount of drug not incorporated. The following equation is used to calculate the AE:

$$AE(\%) = \frac{\text{Total amount of drug} - \text{Free drug in supernatant}}{\text{Total amount of drug}} \times 100$$

**Direct method**

As described by Das and co-researchers [58], the freshly prepared formulation, diluted 1:5, was filtered through a 5 µm nitrocellulose membrane filter (Millipore, Ireland) to remove unencapsulated drug crystals. The drugs used in this study have high solubility in methanol, whereas the lipids are insoluble in methanol. Hence, 9 mL methanol was added to a 1 mL filtered formulation and thoroughly mixed to extract the drug from the lipid matrix. The mixture was then centrifuged at 5000 rpm for 15 min and supernatant was filtered through a 0.45 µm PTFE syringe filter (Millipore, Ireland). The supernatant was again diluted 1:1000 with 9 mM phosphate buffer pH3 to the HPLC assay calibration range. The amount of drug in the filtered supernatant was measured by HPLC. The amount of drug in the filtered formulation was then calculated considering the dilution factor. However, this process also measures the unencapsulated drug which is dissolved in the aqueous phase (soluble unencapsulated drug), however camptothecin is practically insoluble in water (2.5 µg/mL) [59], as result the association efficiency was calculated using as below:

$$AE\,(\%) = \frac{Amount\ of\ drug\ in\ the\ filtered\ formulation}{Total\ amount\ of\ drug}\ x\ 100$$

## 3.4. *In vitro* studies

### 3.4.1 Viability studies

The viability of EC, U87 glioma cell line and human astrocytes exposed to camptothecin-loaded SLN, free drug and SLN was assessed by using the AlamarBlue™ assay. The pink-coloured formazan product was quantified by absorbance measurement ($\lambda$ (excitation) = 530 nm, $\lambda$ (emission) = 590 nm) to detect conversion of the dye by mitochondrial dehydrogenases. This assay is based on the ability of mitochondrial dehydrogenase to cleave the tetrazolium rings of an MTT derivative [3-(4,5-dimethylthiazol-2-yl)-2,5-diphenyl-tetrazolium bromide] and to form formazan crystals which are impermeable to cell membranes, therefore resulting in its accumulation within living cells. Before performing the assay, a standard curve must be designed, to know the most suitable cell seeding concentration for the measurements to fall into the assay linear detection range. 100 µL of cell suspension at different cell concentrations were seeded into wells of 96-well tissue culture test plates. After 24h of culturing on a humidified incubator at 37ºC under and 5% $CO_2$ atmosphere, 10% of the culture volume AlamarBlue™ assay were added to the cultures and the plate was incubated for 24 hours at 37ºC, in the dark. And at each time point 2h, 4h and 24h the absorbance were measured. The results were analysed by plotting absorbance versus cell seeding density.

Then, cells were seeded on the most suitable cell densities and incubated during 24 hour. Then, the cells were put in the presence of different formulations (CPT solution, CPT-SLN and unloaded SLN). The SLN formulations were diluted in complete medium to appropriate concentration. For the camptothecin solution, camptothecin was dissolved in DMSO (1mg/mL) and afterwards diluted in complete medium to appropriate concentrations. After 24h of culturing on a humidified incubator at 37ºC under a 5% $CO_2$ atmosphere, 10% of the culture volume AlamarBlue™ assay were added to the cultures and the plate was incubated at 37ºC, in the dark and metabolic cell activity was measured for the following 2–24 h. The absorbance was measured on the multiwall plate reader and was expressed as % of control

## Statistical Analysis

Statistical analysis were performed using GraphPad Prism 4.0; GraphPad Software, San Diego, CA, USA. ANOVA were performed to compare two or multiple independent groups. Then, a multiple comparison test were used. Results are reported as mean ± standard deviation (SD) from a minimum of three independent experiments. When the group was significantly different, $p<0.01$.

# Chapter 4

# Results & Discussion

In recent years, it has been clear that the BBB is more than a simple barrier. It is composed by a complex neurovascular unit and soluble factors, all these conditions can have an impact on the barrier integrity and function. Specifically, in pathological conditions such as brain tumor and Alzheimer's disease where there are a loss of BBB characteristics. Even though, the most crucial limitation in diagnosis and treatment of these diseases is the unique and complicated environment imposed by BBB. So far, as BBB as a critical obstacle, there are not an effective treatment [7]. As a result, how the BBB could be influenced by various pathogenic or drug factors using different simultaneous studies of various cell types (astrocytes and EC) and fluid phase factors (adhesion molecules and proinflammatory factors), it can be an important solution to increase the minimal ingress through the BBB of potential anti-cancer drugs [15].

In following decades, the *in vitro* model has become a powerful mainstay tool for studying all this alterations. Since, it has a simple structure, a controlled environment and it can be possible create different cell cultures configurations as well as study different parameters at the same time. However, at present, no *in vitro* model can faithfully reproduce all the properties and characteristics of the *in vivo* BBB.

Thus, a semi-permeable plate filter BBB model using human EC has been improved. Firstly, it was performed an *in vitro* model using endothelial mouse cells and astrocytes cells, to improve laboratory skills and understand better the mechanisms involved on this static model. Then, different *in vitro* models using three different type of human cells were established and numerous parameters were studied, specifically to provide a system that could be used to assess the permeability of anti-cancer drugs (CPT drug) and study BBB functions and biological interactions.

## 4.1. Characterization of the *in vitro* mouse model

To have a first contact on the *in vitro* models methodology, it was performed monocultures and co-cultures using primary mouse astrocytes cells and bEnd3 cell line. Li and co-researchers [47] have been exploring the impact of different types mouse BBB cells and various basement membrane coatings can have on the barrier integrity. Regarding this work, it was tested two different endothelial initial concentrations to understand how the densities of the cells can influence its integrity during the time, Figure 4.1. On day 7, the endothelial monolayer achieved the highest TEER values at $0.9x10^5$ cells/cm$^2$ initial concentration. After, this day, the cells became senescent in both concentrations and TEER values decrease which indicates the loss of barrier integrity.

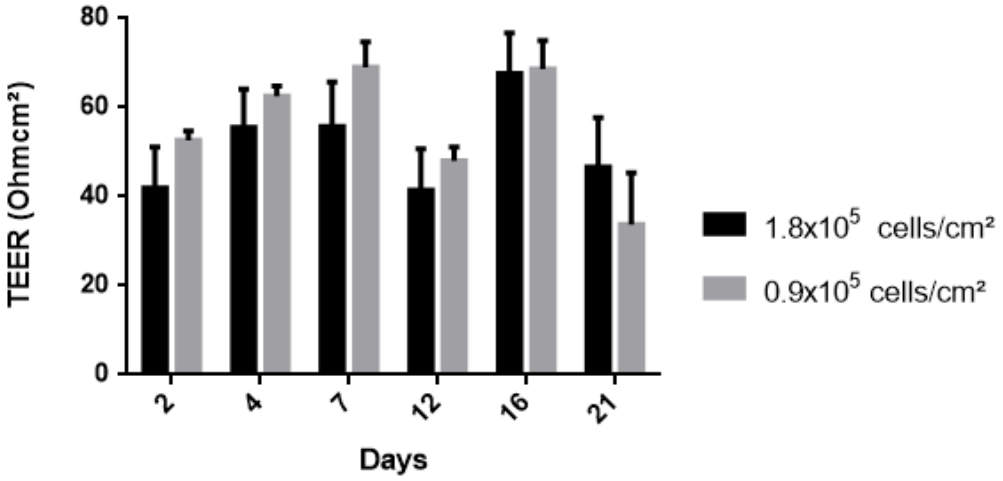


**Figure 4.1** TEER_measurements in different cell mouse densities on monoculture. The resistance value (Ω×cm$^2$) of an empty filter was subtracted from each measurement. Three measurements were taken per filter, and each culture condition was performed with triplicate filters to obtain average TEER and standard deviation. ANOVA showed no significant differences between $1.8 \times 10^5$ cells/cm$^2$ and $0.9 \times 10^5$ cells/cm$^2$ TEER measurements over time.

Moreover, it was study the methodology to establish co-cultures using primary rat astrocytes on the on the inverted side of the semi-permeable filter. Also, it was assessed its impact on the barrier integrity by immunocytochemistry using tight junction markers, permeability assays using an compound with low molecular weight and TEER measurements [data not shown]. The TEER values with astrocytes increase, however, do not showed significant differences, the same results to permeability assay.

Consequently, these first study was important to establish laboratory techniques and different approaches that were applied to the following *in vitro* models. Also, it was an opportunity to explore this new concept while orders were taken and all laboratory material and equipment necessary arrived.

## 4.2. Characterization of the in vitro human BBB model on monoculture

The hCMEC/D3 cell line shows a stable phenotype, expression of endothelial cell markers, tight junction molecules, chemokine receptors and ABC-transporters. Furthermore, the paracellular permeability is much lower compared to other cell lines. These characteristics make the hCMEC/D3 an interesting tool for permeability studies and a long-lasting source of human brain EC to test [15, 48, 54]. Moreover, it will be a better solution to use human cells, to mimic the BBB *in vivo,* than use mouse cells.

To the purpose of endothelial human cells function as a barrier, it is essential that they create a confluent monolayer with tight junction between the EC [60]. First of all, it was used different cellular concentrations and it was analyzed its integrity by TEER measurements, monitoring it over the time in cell culture. The barrier model has TEER values ranged between 0.9–32 $\Omega/cm^2$. The highest TEER value was achieved with an initial $4.6x10^4$cells/$cm^2$ cell concentration and with 7 days of culture, Figure 4.2.

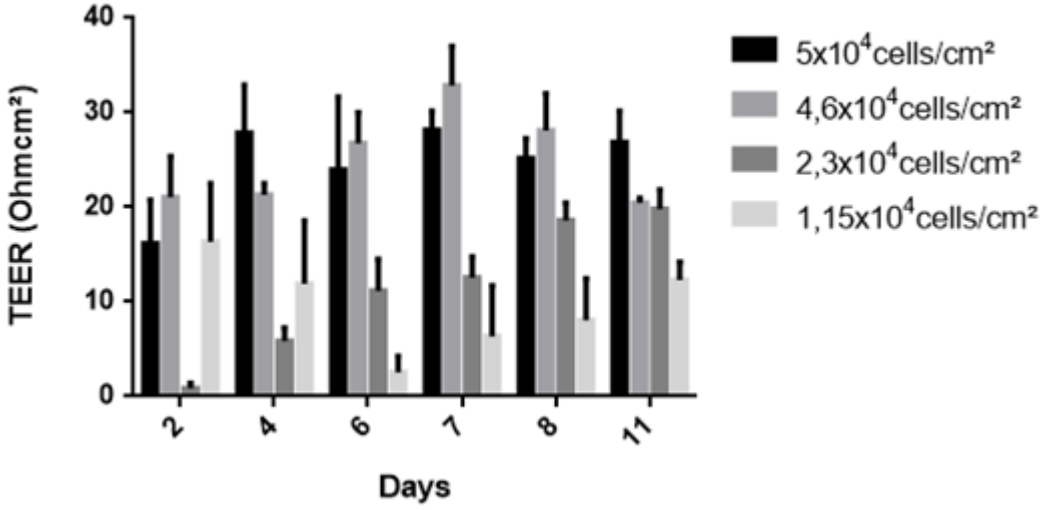


**Figure 4.2** TEER measurements in different cell human densities on monoculture. The resistance value ($\Omega \times cm^2$) of an empty filter was subtracted from each measurement. Six measurements were taken per filter, and each culture condition was performed with triplicate filters to obtain average TEER and standard deviation. ANOVA showed differences of TEER values on 2nd day at 5 x $10^4$ cells/$cm^2$ versus 2.3 x $10^4$ cells/$cm^2$ (*), at 4.6 x $10^4$ cells/$cm^2$ versus 2.3 x $10^4$ cells/$cm^2$ (**) and at 2.3 x $10^4$ cells/$cm^2$ versus 1.15 x $10^4$ cells/$cm^2$ (*); on 4th day at 5 x $10^4$ cells/$cm^2$ versus 2.3 x $10^4$ cells/$cm^2$ (***), at 5 x $10^4$ cells/$cm^2$ versus 1.15 x $10^4$ cells/$cm^2$ (*) and at 4.6 x $10^4$ cells/$cm^2$ versus 2.3 x $10^4$ cells/$cm^2$ (*); on 6th day at 5 x $10^4$ cells/$cm^2$ versus 1.15 x $10^4$ cells/$cm^2$ (***), at 4.6 x $10^4$ cells/$cm^2$ versus 2.3 x $10^4$ cells/$cm^2$ (**), at 4.6 x $10^4$ cells/$cm^2$ versus 1.15 x $10^4$ cells/$cm^2$ (***); on 7th day at 5 x $10^4$ cells/$cm^2$ versus 2.3 x $10^4$ cells/$cm^2$ (*), at 5 x $10^4$ cells/$cm^2$ versus 1.15 x $10^4$ cells/$cm^2$ (***), at 4.6 x $10^4$ cells/$cm^2$ versus 2.3 x $10^4$ cells/$cm^2$ (**), at 4.6 x $10^4$ cells/$cm^2$ versus 1.15 x $10^4$ cells/$cm^2$ (****); on 8th day at 5 x $10^4$ cells/$cm^2$ versus 1.15 x $10^4$ cells/$cm^2$ (**) and at 4.6 x $10^4$ cells/$cm^2$ versus 1.15 x $10^4$ cells/$cm^2$ (**); on 11th day at 5 x $10^4$ cells/$cm^2$ versus 1.15 x $10^4$ cells/$cm^2$ (*). At 4.6 x $10^4$ cells/$cm^2$ there are statistical significant differences (*) between the 7th day and 11th day. * ($p \leq 0.05$) indicates statistical significant differences; ** ($p \leq 0.01$) indicates very statistical significant differences; *** ($p \leq 0.001$) indicates extremely significant statistical differences and **** ($p \leq 0.0001$) indicates extremely significant statistical differences.

The TEER values obtained were lower than those usually obtained *in vivo* (1500-8000 $\Omega cm^2$). TEER values higher than 1000 $\Omega cm^2$ are really difficult to achieve on the *in vitro* cell culture model, specially for immortalized cell lines compared to primary cells. Nevertheless, the TEER values obtained are in agreement with recent publications, under static culture conditions the values are around 40 $\Omega cm^2$ [60, 61]. However, there are some strategies that can be used to increase TEER values, such as increasing hydrocortisone (anti-inflammatory steroid) concentration can influence the expression of TJ proteins and increase TEER values close to 300 $\Omega cm^2$ [62], added different cells types to mimicking the neurovascular unit or applied flow based shear stress, the TEER reported achieved 1000-1200 $\Omega cm^2$ [15, 48].

Moreover, on the last days, $8^{th}$ and $11^{th}$, the TEER values are decreasing which indicates that the cells became senescent and the barrier is disrupted. As a result, besides the low TEER values, it was proven that the hCMEC/D3 monolayer do reflect an intact and functional barrier at 4.6 x $10^4$ cells/$cm^2$ as initial concentration. Furthermore, the TEER values are, in all experiences, very similar which indicates a reproducible approach to study the BBB.

Besides the TEER analysis, the membrane integrity was evaluated by optical microscopy giemsa technique, Figure 4.3, and by observation of membrane markers, WGA-Alexa Fluor 488, using immunocytochemistry technique, Figure 4.4. Both analysis were performed at different time points, on $2^{nd}$, $4^{th}$, $7^{th}$, $9^{th}$ and using 4.6x$10^4$ cells/$cm^2$ as initial concentration.

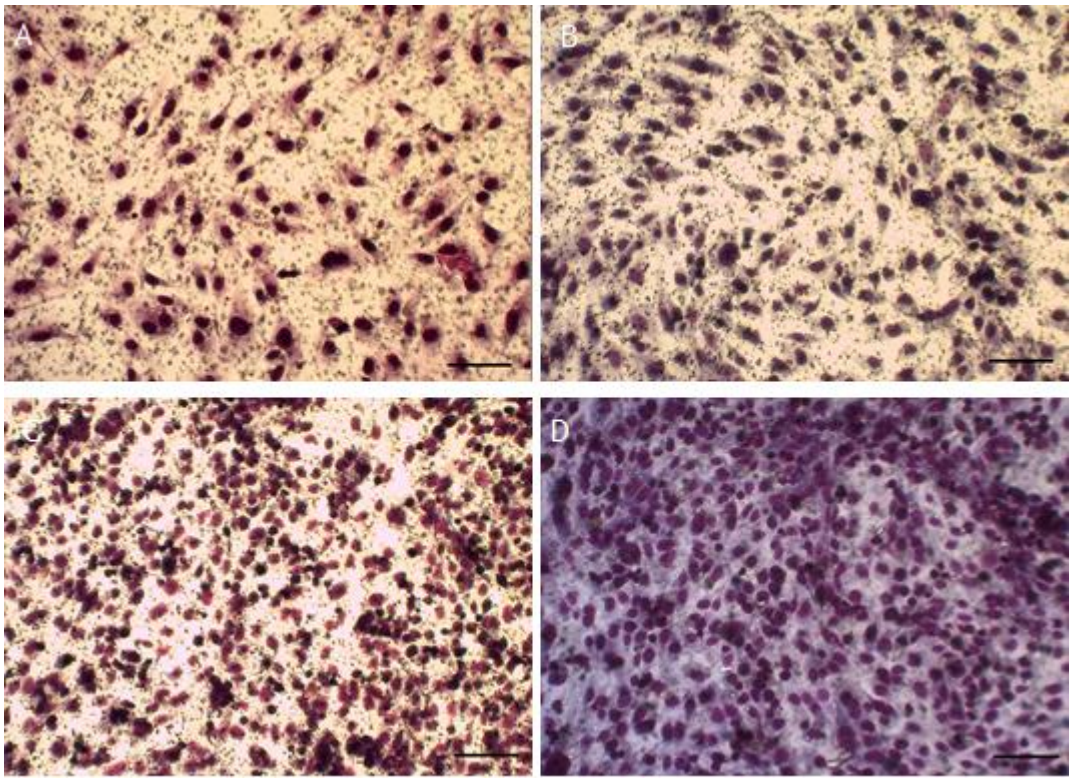


**Figure 4.3** Phase contrast microscopy observation of an endothelial-enriched human culture with giemsa staining grown on semi-permeable filters with 200x magnification. A. 2nd day. B. 4th day. C. 7th day. D. 9th day. Bar = 50 µm.

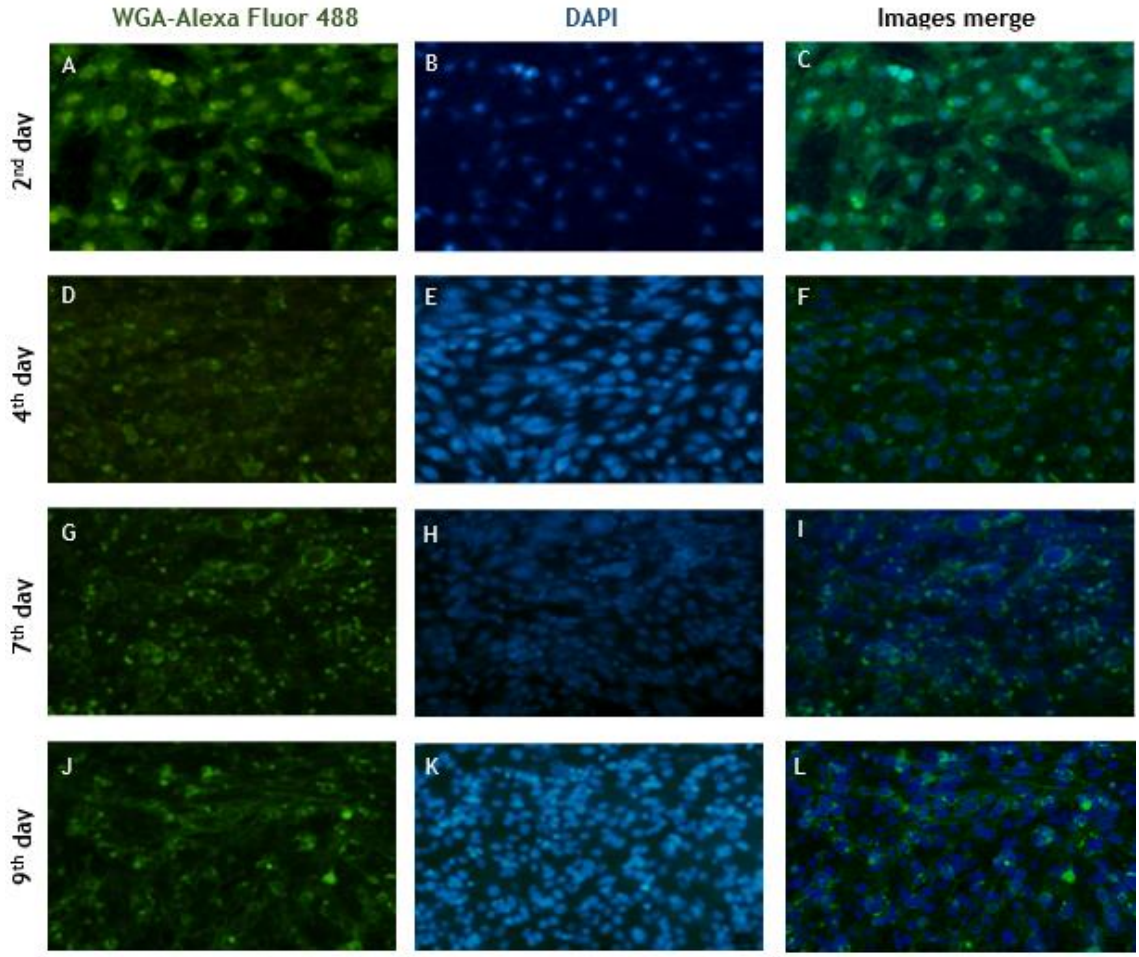


**Figure 4.4** Immunofluorescence labeling endothelial-enriched culture with DAPI (nucleus dye) and Alexa Fluor-488 WGA (plasma membrane dye) grown on semi-permeable filters with 200x magnification. A-C. 2nd day. D-F. 4th day. G-I. 7th day. J-L. 9th day. E. 11th day. Bar= 10 µm.

Without a doubt, the images from both techniques showed, on initial stages - 2nd and 4th days, the presence of spaces with low cellular interactions, which indicates the normal cellular growth on semi-permeable filters. On the other hand, on last day, Figure 4.3-D and figure 4.4-J to L, the cells present a random pattern known as "edge effect" and became senescence. Consequently, there are an alteration on barrier integrity which is in agreement with the decreasing of TEER values over the time. Finally, on 7th day, the cells form a monoculture with very few gaps and high cellular interactions indicating that this is the day where the cells form a confluent monolayer and the barrier maintains its integrity. However, it is necessary to study specific endothelial specific markers to analyze if barrier presents a highly restrictive barrier and also to study the localization of tight junction markers.

Therefore, to guarantee the phenotype of this endothelial cell line, on the 7th day and using $4.6x10^4$ cells/$cm^2$ as initial concentration, the expression of endothelial specific markers were analyzed by flow cytometry, Figure 4.5. Also, the expression of TJ proteins as well as adhesion junctions where analyzed by immunostaining, Figure 4.6.

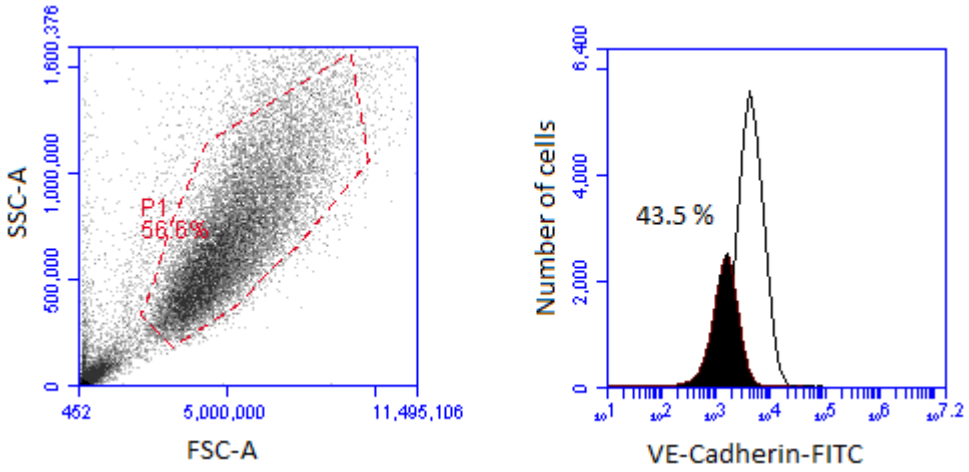


**Figure 4.5** Cellular gate and fluorescence histogram from hCMEC/D3 flow cytometry experiment using VE-Cadherin-FITC. [A] The dotted red line indicates the gate for individual hCMEC/D3 cells. Establishing this gate excludes debris (lower left) and aggregated cells (upper right) from analysis. [B] Gray tracks are negative controls, corresponding to staining in the absence of the antibody marker, while tracks in black are specific staining for the indicated adhesion marker.

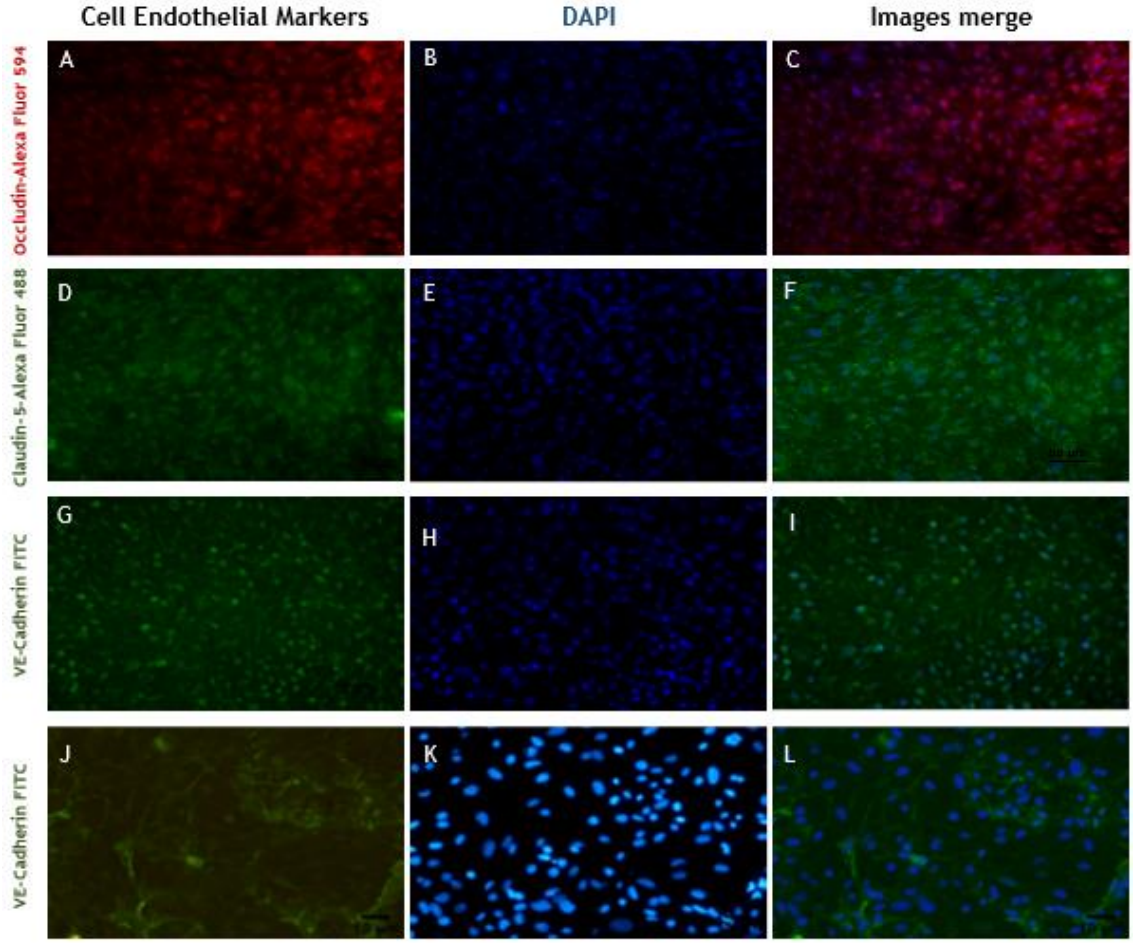


**Figure 4.6** Immunofluorescence images. Immunofluorescence labeling endothelial-enriched culture with DAPI and A-C Occludin-Alexa Fluor 594; D-F Claudin-5-Alexa Fluor 488; G-I VE-Cadherin-FITC grown on semi-permeable filters at 200x magnification Bar=50 µm. J-L VE-Cadherin-FITC at 400x magnification on coverslip cell culture.

The three proteins tested are well characterized endothelial markers, VE-Cadherin is an adhesion junction marker present on the majority of EC and Occludin and Claudin-5 is expressed where a tight junction is established. For this reason, this three markers can be good indicators to evaluate the barrier of the *in vitro* model. However, occludin and claudin-5 markers are important to guarantee EC phenotype and barrier integrity, this cell line showed lower expression of claudin-5 and occludin [63].

Concerning to flow cytometry analysis around 44 % of the cells are expressing the endothelial specific marker. These are immortalized cells which had been submitted to some modifications which can influence the expression of some markers over the time in culture, however these values are consistent. By contrast, hCMEC/D3 cells were not stained by markers specific for other brain cells, specifically GFAP (astrocytes cells), which guarantee its phenotype [data not shown].

Moreover, on Figure 4.6 – C and Figure 4.6 - F show a pure endothelial culture as occludin and claudin-5 staining can be noticed in the majority of all DAPI-stained cells, showing the TJ established. Also, on Figure 4.6 – G VE-Cadherin is expressed for all endothelial culture. However, on Figure 4.6 – L, VE-Cadherin on coverslip culture in higher magnification, it is more evident the endothelial monoculture well organized and continuous cell-cell borders, as well as very few gaps on the membrane filter. It seems that the semi permeable filter have an impact on the background of the image which is not visible when stained in coverslips.

Also, the low expression of tight junction markers can be due to the lack of astrocytes on culture that are important to maintain BBB phenotype. The astrocytes produce different members of the Wnt family which increase the expression of junctional proteins. Even, on the endothelial medium were added different compounds, hydrocortisone and lithium chloride (Wnt/ß-catenin signaling activator) [64], as well as bFGF that can enhance expression of junctional proteins [48]. These compounds could not be present on the same concentrations. Therefore, increasing or modulating these three compounds can influence the expression of tight junction markers and improve the growth of this cell line on the *in vitro* cellular model [48].

Finally, it was performed permeability assays using three compounds with different MW. The compounds crossed the semi-permeable filter with different rates during 150 minutes, through the EC monolayer, Figure 4.7 – A, and through the “blank” filter i.e. the filter coated with rat tail collagen type I without any cellular barrier, Figure 4.7 – B. The FD4, FD40 and FD70 are used as a marker of paracellular permeability.

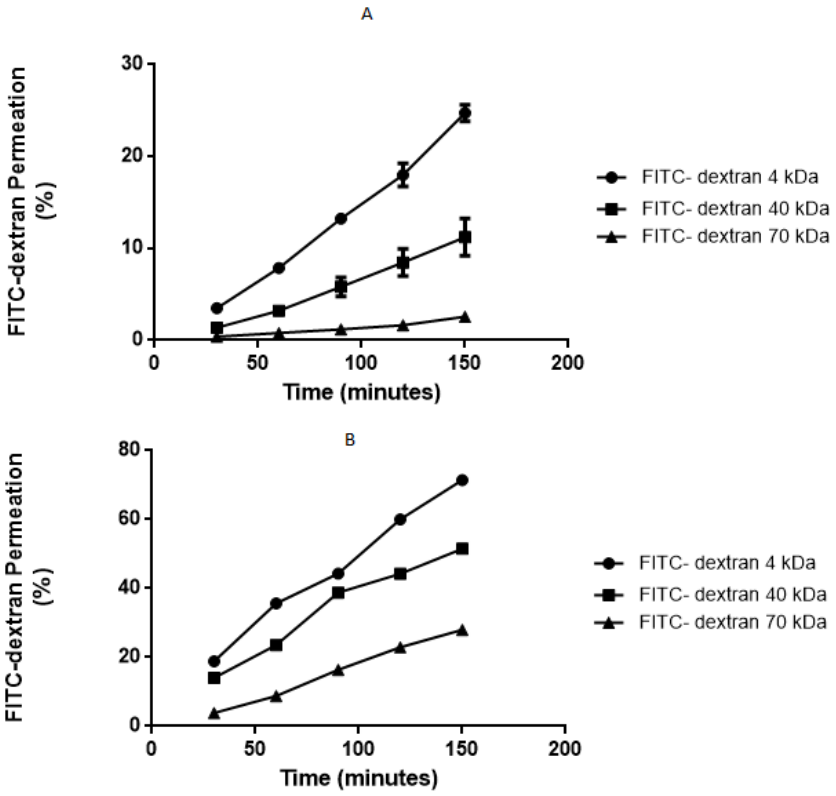


**Figure 4.7** Permeability assay. Permeability experiment were taken at 7th day, FD4, FD40 and FD70 crossed the endothelial barrier. [A] Through the cell monolayer. [B] Through the blank filter.

Considering the "blank filter" permeability values, it is clear that it has an impact on the experiment, as initially 500 µg applied to the luminal side of the filter, 357 µg – 71% FD4, 257 µg – 51 % FD40 and 139 µg – 27% FD70 crossed to the abluminal side. It is also evident that the EC decrease this permeability, approximately only 120 µg – 24% for FD4, 56 µg – 11 % for FD40 and 13ug – 2.56% for FD70 can be able to cross the endothelial barrier.

As referred to apparent permeability the values are for FD4 is 15.3 ± 0.6x$10^{-6}$ cm/s, for FD40 is 6.9 ± 1.2x$10^{-6}$ cm/s and for FD70 is 1.6 ± 0.2x$10^{-6}$ cm/s, during the assay TEER values was found to remain constantly. These values are similar to published data, concerning to FD4 compound, Ragnaill and co-researchers achieved values around 5.5x$10^{-6}$ cm/s [60], Wekler group around 6x$10^{-6}$ cm/s [54] and finally Forster and colleagues achieved higher permeability values around 13x$10^{-6}$ cm/s [62]. In comparison with rat cells using the same compound, higher permeability values are achieved, the values are 16.3x$10^{-6}$ cm/s. Finally, for bovine brain EC on monoculture the values are very similar, 7.2x$10^{-6}$ cm/s to the human EC on monoculture [54].

These values showed that the *in vitro* BBB model on monoculture represents a highly restrictive barrier and the hCMEC/D3 cell line exhibits a higher paracellular resistance. So, it indicates that the model can be used to study CPT-SLN permeation.

## 4.3. The influence of different cells on the *in vitro* BBB model

Recent studies have been shown that the increase of the complexity of the model can be improve the integrity and reproduce better the BBB *in vivo*. So, it is clear that perform co-cultures with different cell types and various factors can be a good strategy to study better the BBB. In this way, it was added to the last model, primary astrocytes and a glioma cell line and both at the same time to study the impact on TEER resistance, paracellular permeability, expression of endothelial cell markers and endothelial surface.

Before to perform the *in vitro* models set-up, it was analyzed the cellular growth until the confluence stage on cell culture flasks and on semi-permeable filters. Also, it was analyzed various published approaches where human cells were used or where it was used the same methodology.

Concerning to EC co-cultured with the glioma cell line, it had been in consideration that on $2^{nd}$ day the EC are already seeded on the semi-permeable filter and expressing TEER values around 18 $\Omega cm^2$. The glioma cells were seeded on the bottom of the abluminal side based like reported for other researchers [65]. Mainly, the impact of the glioma on the EC is from the factors released on the cellular medium as recently Dwyer and co-researchers [66] showed. Thus, the glioma cell line was seeded the on $2^{nd}$ day and co-cultured performed during the follow five days.

Regarding to EC co-cultured with primary astrocytes, it has been in attention that primary astrocytes growth it is much lower than EC one, in order to leave them to establish without any environment interaction, these cells were seeded first. Astrocytes were seeded on the inverted side on the filter, as reported by [47] and [15], to create possible mechanical interactions which can influence the EC characteristics and develop an *in vitro* model more close that what happens *in vivo*. Then, to maintain the endothelial monoculture set-up, it was added the EC after the astrocytes are on semi-permeable filter. The initial astrocytes concentration, it not in agreement with other works mainly due to the cellular limitation and low growth. Finally, the co-cultures were maintained during the follow seven days.

The last model, where it was used the three cell types, were established using the last ideas.

Firstly, it was study the integrity barrier in the three different conditions by TEER measurements. To illustrate the main differences it was separate the three conditions in three independent graphs. Figure 4.8 refers to EC co-cultured with U87 glioma cell line. Figure 4.9 indicates the impact the astrocytes cells have on EC. And then, on figure 4.10 is possible analyze the TEER values differences between the three *in vitro* models purposed.

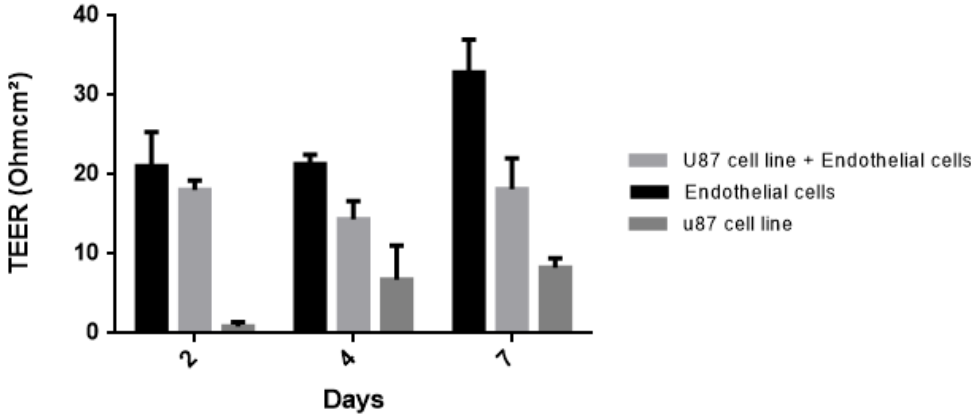


**Figure 4.8** TEER measurements in co-culture, endothelial cells and U87 cell line. The resistance value ($\Omega \times cm^2$) of an empty filter was subtracted from each measurement. Six measurements were taken per filter, and each culture condition was performed with triplicate filters to obtain average TEER and standard deviation. ANOVA showed differences of TEER values on 2nd day, at Endothelial cells versus U87 cell line (***); on 4th day at Endothelial cells versus U87 cell line (**); on day 7th day at Endothelial cells versus U87 cell line (****), Endothelial cells versus Endothelial cells + U87 cell line (**) and Endothelial cells + U87 cell line versus U87 cell line (**). At Endothelial cells there are statistical significant differences (*) between the 4th day and 7th day. * ($p \leq 0.05$) indicates statistical significant differences; ** ($p \leq 0.01$) indicates very statistical significant differences; *** ($p \leq 0.001$) indicates extremely significant statistical differences and **** ($p \leq 0.0001$) indicates extremely significant statistical differences.

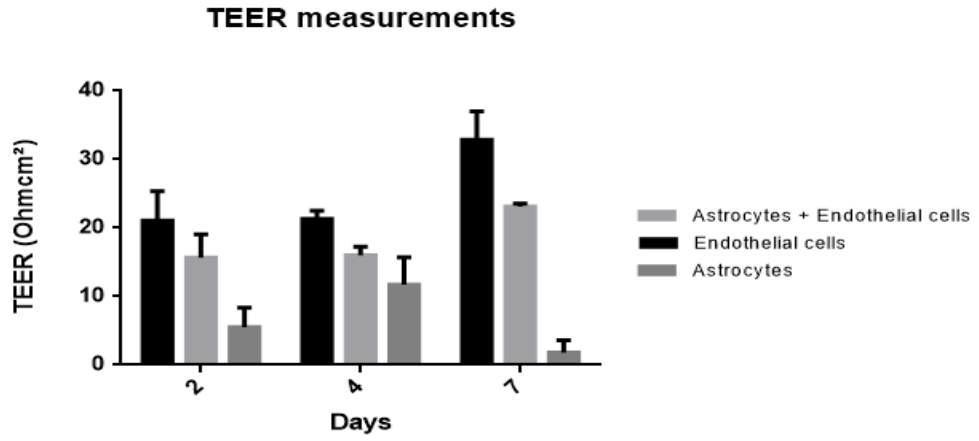


**Figure 4.9** TEER measurements in co-culture, endothelial cells and primary astrocytes cells. The resistance value ($\Omega \times cm^2$) of an empty filter was subtracted from each measurement. Six measurements were taken per filter, and each culture condition was performed with triplicate filters to obtain average TEER and standard deviation. ANOVA showed differences of TEER values on 2nd day, at Endothelial cells versus astrocytes (**); on day 7th day at Endothelial cells versus Astrocytes (****), Endothelial cells + Astrocytes versus Astrocytes (***) and Endothelial cells + Astrocytes versus Endothelial Cells (*). At Endothelial cells there are statistical significant differences (*) between the 4th day and 7th day. * ($p \leq 0.05$) indicates statistical significant differences; ** ($p \leq 0.01$) indicates very statistical significant differences; *** ($p \leq 0.001$) indicates extremely significant statistical differences and **** ($p \leq 0.0001$) indicates extremely significant statistical differences.

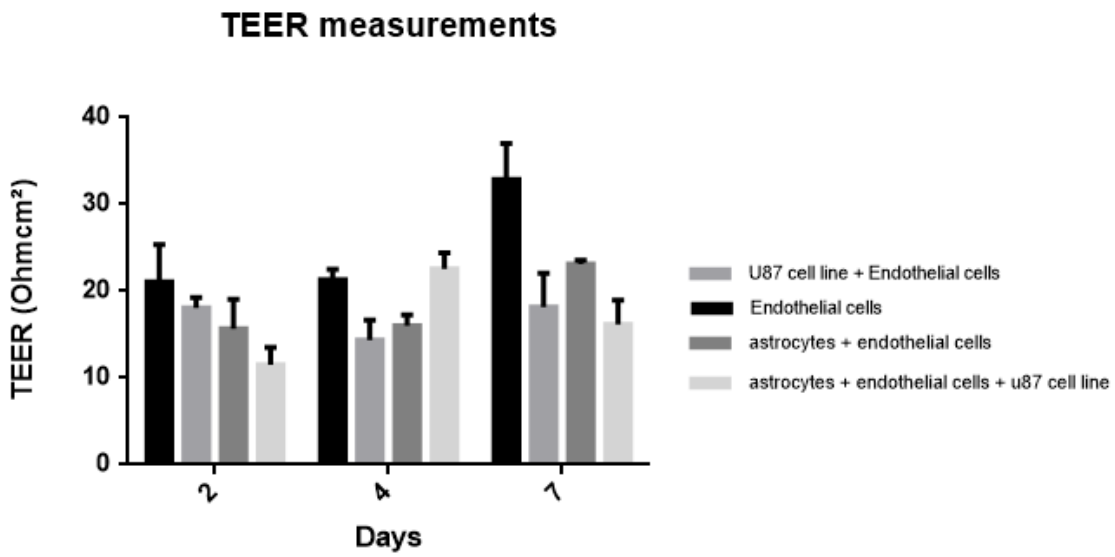


**Figure 4.10** TEER measurements in endothelial cells cultured with U87 cell line and primary astrocytes cells. The resistance value ($\Omega \times cm^2$) of an empty filter was subtracted from each measurement. Six measurements were taken per filter, and each culture condition was performed with triplicate filters to obtain average TEER and standard deviation. ANOVA showed differences of TEER values on 2nd day, at Endothelial cells versus Endothelial cells + Astrocytes + U87 cell line (*); on 7th day at Endothelial cells versus Astrocytes + Endothelial Cells (*), Endothelial cells versus U87 cell line (**) and Endothelial Cells versus Endothelial cells + Astrocytes + U87 cell line (***). At Endothelial cells there are statistical significant differences (*) between the 4th day and 7th day. * ($p \leq 0.05$) indicates statistical significant differences; ** ($p \leq 0.01$) indicates very statistical significant differences and *** ($p \leq 0.001$) indicates extremely significant statistical differences.

Then, it was chosen FD4 molecule to perform permeability assays due to the high crossed flux on the endothelial monoculture, Figure 4.11.

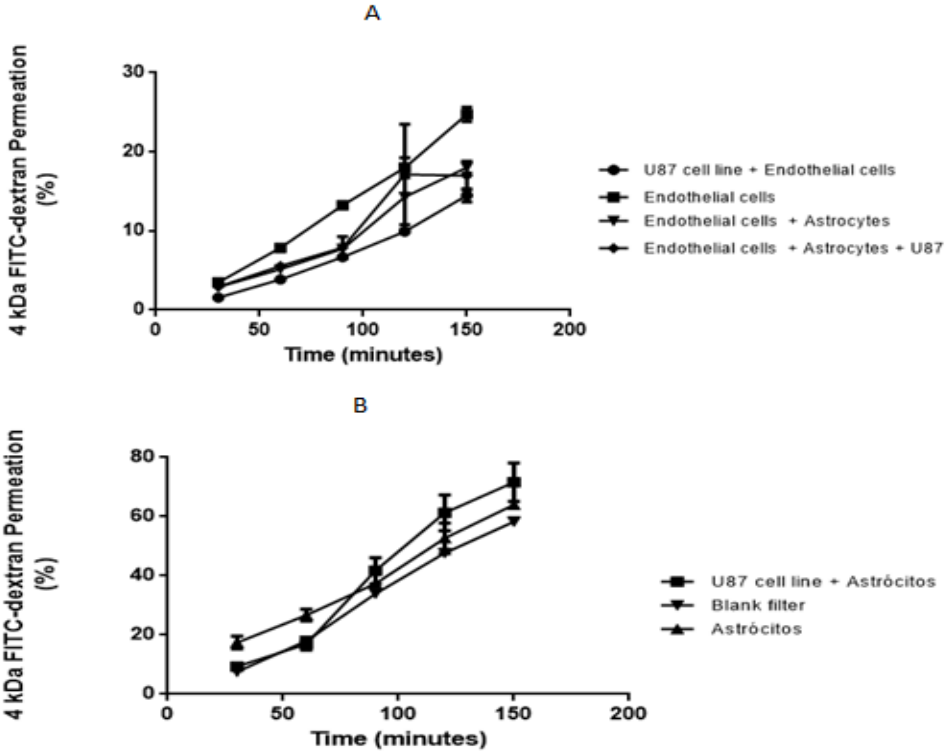


**Figure 4.11** Permeability assay on 7th day. Permeability experiment using the FD4 molecule. [A] Through the different cell cultures, endothelial cells, U87 cell line and endothelial cells, endothelial cells and astrocytes and finally, endothelial cells, astrocytes and U87 cell line [B] Through the controls filters, U87 cell line and astrocytes, the blank filter without any cells and astrocytes.

As expected, glioma cell line presence decreased TEER values and integrity barrier is affected, figure 4.8. The apparent permeability values for this cellular condition was 8.9 ± 0.5x$10^{-6}$ cm/s and around 14% FD4 crossed the cellular membrane. As said before, the FD4 apparent permeability on the monoculture was 15.3 ± 0.6x$10^{-6}$ cm/s. In comparison with reported works as [66], there are 2.5 fold augmentation of the FD40 apparent permeability to compared with the negative condition, the serum free media. However, in this study it was used only the conditioned medium. And in the model purposed, the glioma cells are seeded on the bottom which can influence the sample collect. For this reason, the permeability values with glioma cells presence are not so higher as has been expected, Figure 4.11.

According to astrocytes effect, no significant differences were observed in TEER values between endothelial cells and EC co-cultured with human astrocytes, Figure 4.9. However, thus it has already been confirming by Poller and co-workers [67] and Weksler and co-researchers [48], which indicates that this cell line is capable to form an tight barrier even without astrocytes cells. In contrast of Hatherell work [49] that showed significant difference to use astrocytes in co-culture with EC. The main reason for this opposite opinion can be the serum supplementation or the astrocytes cells used to be different.

On permeability experiment seems that astrocytes alone do not influence the integrity of the barrier as well as the astrocytes co-cultured with EC, Figure 4.11. The apparent permeability was 7.6 ± 6.1x$10^{-6}$ cm/s and around 18% FD4 crossed the barrier. Though, this results can be a consequence of the low initial cellular concentration that cannot be sufficient to influence EC.

Finally, when comparing the *in vitro* model with three cells, it is clear that astrocytes are not able to reduce the U87 cell line effect on the TEER values, Figure 4.10. Also, in this condition, EC remain the model with higher TEER values. Concern to the permeability values, the apparent permeability was 10.5 ± 1.1x$10^{-6}$ cm/s and around 16% FD4 crossed, Figure 4.11, which is in agreement with the TEER values decreasing.

To understand better the impact the U87 cell line on the barrier, it was performed immunocytochemistry and flow cytometry analysis. In case of immunocytochemistry it was tested occludin, VE-cadherin and claudin-5. The images taken showed unspecific bound [data not shown]. On flow cytometry studies were tested VE-cadherin FITC, since VE-Cadherin plays an important rule on leukocyte extravasation, Figure 4.12.

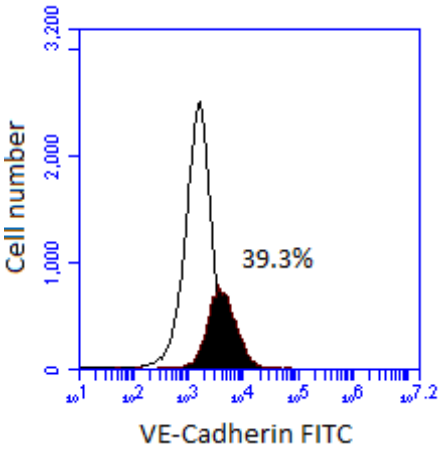


**Figure 4.12** Fluorescence histogram from hCMEC/D3 co-cultured with U87 cell line using VE-Cadherin-FITC. Gray tracks are negative controls, corresponding to staining in the absence of the antibody marker, while tracks in black are specific staining for the indicated adhesion marker.

As expected the VE-Cadherin expression is affected [66], which indicates the VE-Cadherin mediated cell-cell junctions alteration during the time exposed to U87 cell line released factors. However, tested at different time points it will be necessary to proven its remodeling during the time exposed to the inflammatory factors released by U87 cell line. Moreover, it was analyzed endothelial and astrocyte surface by SEM, Figure 4.13, 4.14 and 4.15.

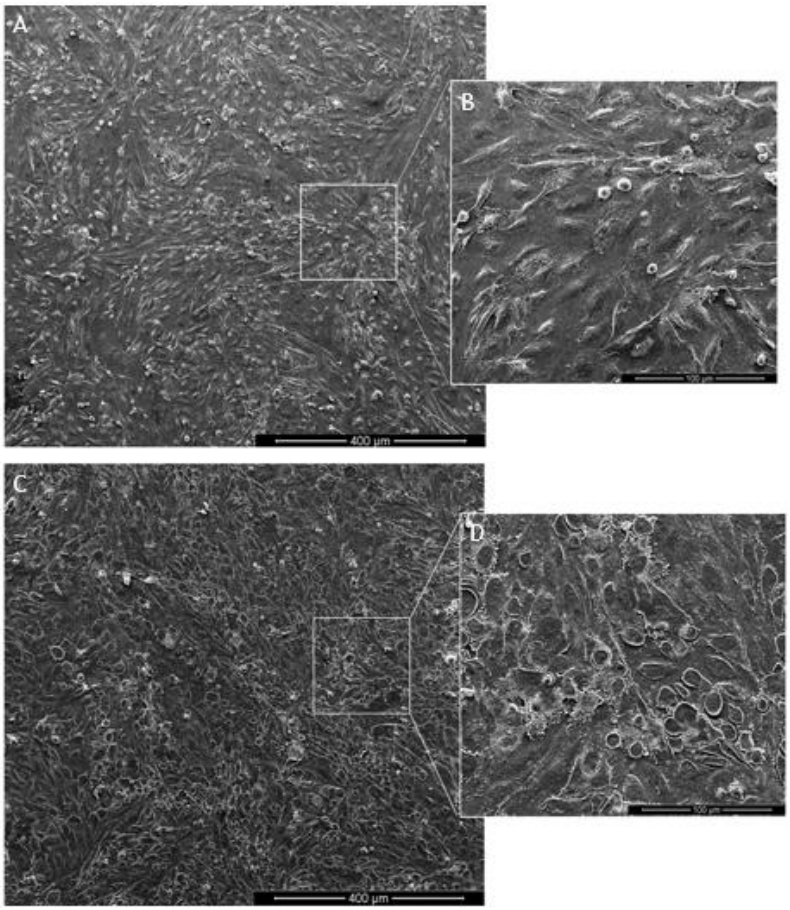


**Figure 4.13** SEM images of surface endothelial cells co-cultured with astrocytes and U87 cell line on 7th day. [A] Endothelial cells with astrocytes at 250 x magnification. [B] Endothelial cells with astrocytes at

1000 x magnification. [C] Endothelial cells on co culture with U87 cell line at 250 x magnification. [D] Endothelial cells on co culture with U87 cell line at 1000 x magnification.

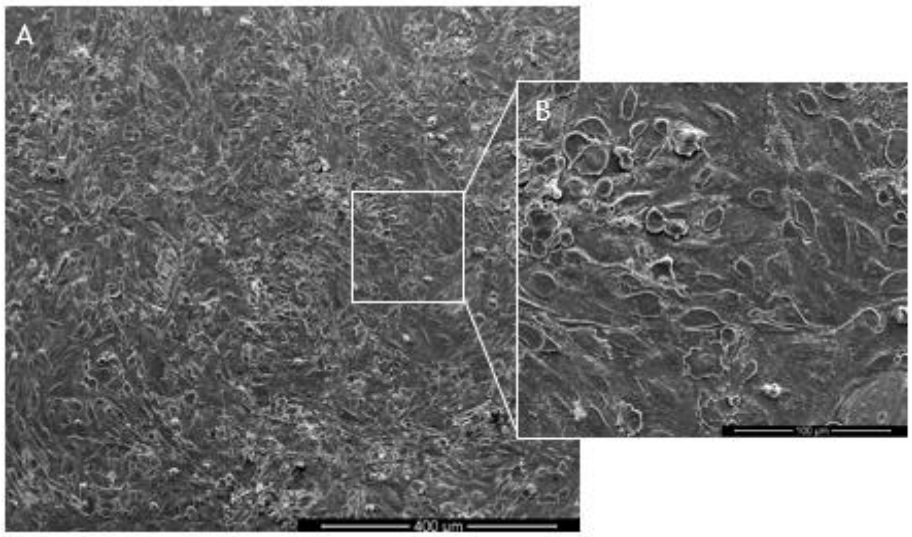


**Figure 4.14** SEM images of endothelial cells surface co cultured with astrocytes and U87 cell line in on 7th day. [A] Endothelial cells with astrocytes and U87 cell line at 250 x magnification. [B] Endothelial cells with astrocytes and U87 cell line at 1000 x magnification.

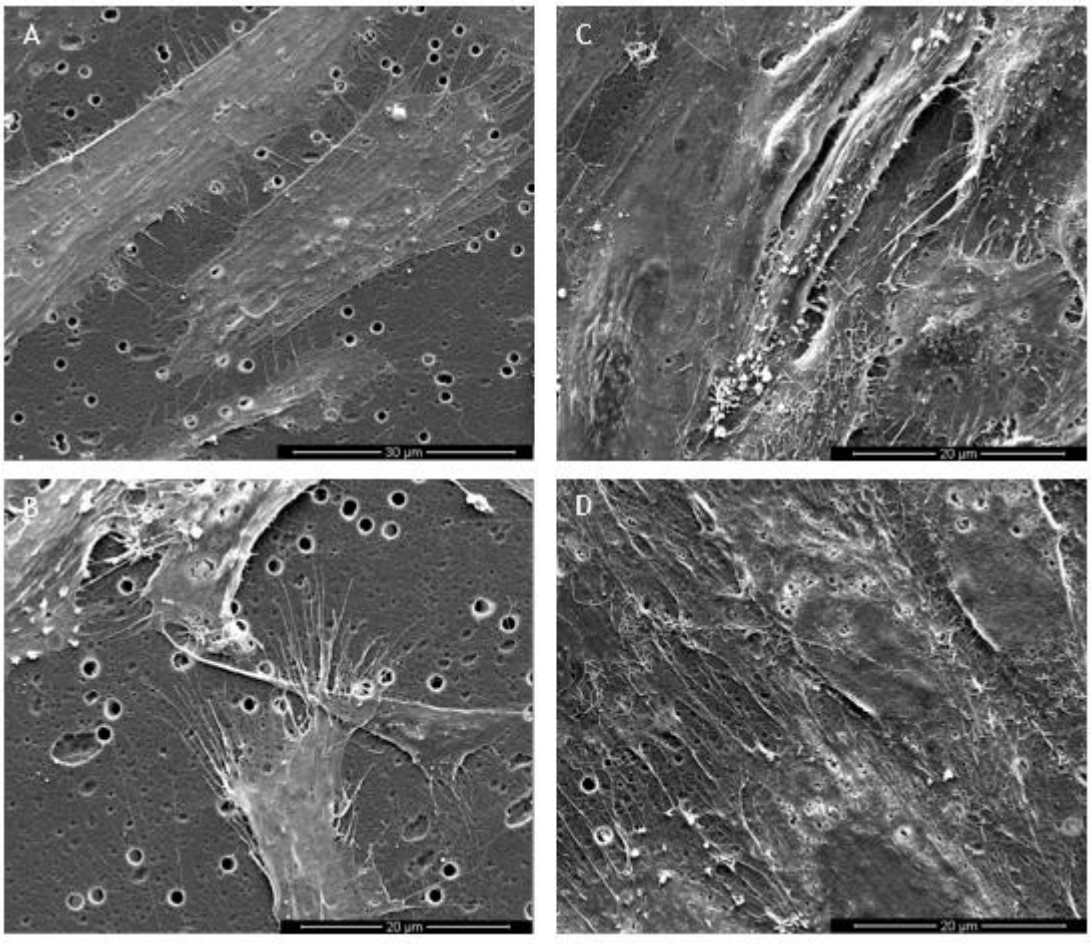

**Figure 4.15** SEM images of endothelial cells, astrocytes and U87 cell line in culture on 7th day. [A] Astrocytes surface co-cultured with endothelial cells seeded on the semi-permeable filter coated before with Geltrex at 3500x magnification. [B] Astrocytes surface co-cultured with endothelial cells seeded on the semi-permeable filter coated before with Geltrex at 5000x magnification. [C] Endothelial cells surface co-cultured with astrocytes at 5000x magnification. [D] Endothelial cells surface co-cultured with astrocytes and U87 cell line at 5000x magnification.

In agreement with last results, Figure 4.13–A and B and Figure 4.15-C clearly illustrates the growth of a confluent endothelial layer. The EC form a confluent monolayer with adjacent growth, with direct cellular interaction which promotes a highly restrictive barrier.

On the other hand, U87 cell line changes cell morphology, Figure 4.13 – C and D, and TJ can be affected and damaged. In Figure 4.15-D it is possible analyze the semi-permeable plate filter and the membrane porous. Lastly, the EC co-cultured with astrocytes and U87 cell line are not differences in comparison with EC co-cultured with U87 cell line, Figure 4.14. Where continuous to exist a flattening of cell shape.

In last results, it was not demonstrated any influence of astrocytes on the *in vitro* model by the soluble factors that are under normal physiological conditions are released. Hatherel and co-researchers [49] showed that this specific cell line responds better to astrocyte contact rather than the soluble factors released to the astrocytes, which it is happens *in vivo*. Where astrocytes are closely to EC in the NVU. Other studies has the same conclusion, that astrocytes end-feet can crossed the semi-permeable filter and making contact with EC [68].

Figure 4.15-A and B showed that astrocytes have a key feature on mechanical interactions, since it seems that astrocytes long end-feet will cross the membrane for the luminal side. Although, more studies will be need to demonstrate this interaction *in vitro*, for example using transmission electron microscopy.

## *4.4.* Nanoparticles characterization

To nanoparticles can achieve easily the brain and cross the BBB is necessary an average size around 200 nm. Several parameters of the production method can alter the size likewise the time of stirring, time of sonication, sonication intensity and the temperature during the process. Based on work of Martins and co-researchers [57], it was optimized the production conditions to have a reproducible samples before the studies of nanoparticle interaction with cells [data not shown]. Also, experiments with animal models suggest that small (<200 nm), neutral or slightly negatively charged particles can move through tumour tissue [35].

Comparing, CPT average size values using both techniques, there are very similar. According to laser diffraction technique, CPT loading had no marked influence on the SLN size and both loaded and empty SLN presented particle median size (Dv50) around 0.200 µm, Figure 4.16, suitable for cell membrane passage and uptake under normal physiological conditions (mean Dv50 for empty SLN was 0.194 µm ± 0.015 and for SLN-CPT was 0.193 µm ± 0.012). The particle size range is represented as mean Dv90 and mean Dv10, which where respectively 0.506 µm ± 0.139 and 0.086 µm ± 0.005 for empty SLN, 0.772 µm ± 0.128 and 0.087 µm ± 0.005 for SLN-CPT. PI values obtained were lower than 0.2 for all nanoformulations, suggesting that the nanoparticles were in a state of acceptable monodispersity distribution, with low variability and no aggregation.

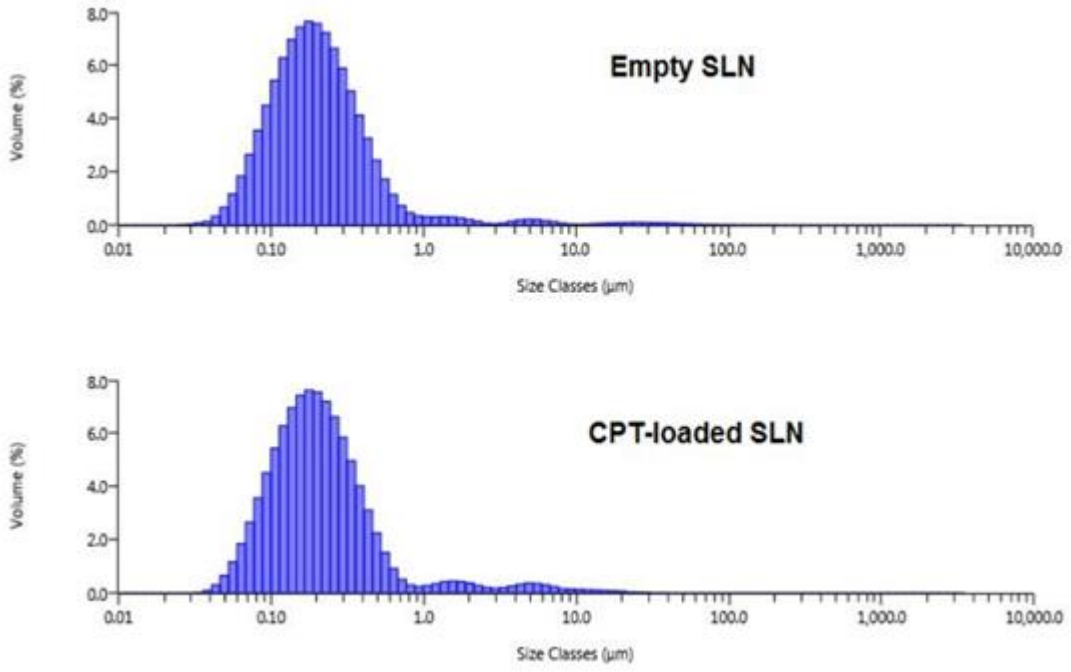


**Figure 4.16** Volume density (%) analysis of Empty and CPT-loaded SLN particle size. Particle size was measured using the laser diffraction particle size analyzer (Malvern Mastersizer 3000, Malvern Instrument, Ltd. It represents at least three independent samples of each sample condition.

SLN also present a negative charge with zeta potential values of -21.27 ± 4.95 mV for empty SLN and -27.14 ± 5.68 for SLN-CPT which indicates a good nanoparticles repulsion and it is avoid nanoparticles agglomeration. Moreover, the drug incorporation seems not affect the nanoparticle charge. Also, the slightly negative charge is favorable to the brain uptake and can be safely used as colloidal drug delivery systems for brain targeting [35].

Before, to calculate the association efficiency it was necessary tested the method validated by Martins and co-researchers [56] by a calibrate curve to correlate the concentration of CPT present on the SLN formulation, Figure 4.17.

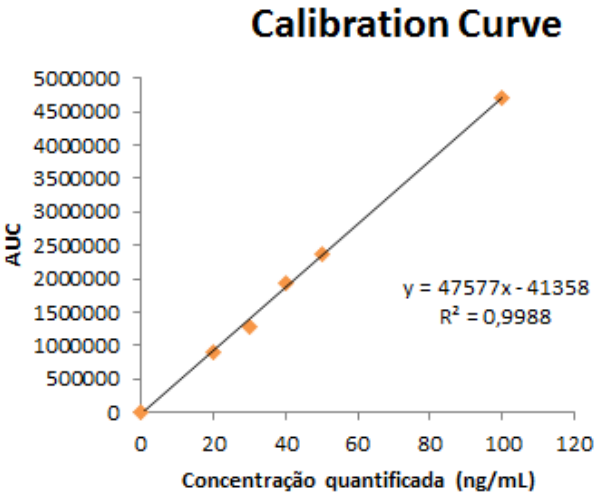


| CPT Concentration (ng/ml) | AUC |
|---|---|
| 0 | 0 |
| 20 | 892496,8 |
| 30 | 1283411 |
| 40 | 1919840 |
| 50 | 2356822 |
| 100 | 4717669 |

**Figure 4.17** Calibration curve to extrapolate CPT concentration values using HPLC method.

Then, it was analyzed the association efficiency using two different methods. Lipid nanoparticles are known to be suitable systems for drug incorporation. Using as Martins and co-researchers [35], the method indirect to determine association efficiency of CPT drug the values obtained were around 98% which indicates a high encapsulation. However, other method were performed to validate the last ones and the values were complete different. In this case, the values obtained were around 11%. As a matter of fact that in the first methodology, the free drug were retained on the centrifuged membrane and it was not solubilized with the water. However, more studies like release studies need to be done to guarantee these association efficiency values.

## 4.5. In vitro studies

Before to perform the viability analysis, it was tested different cellular concentrations and the absorbance were tested at different time points on EC, on glioma cell line and on primary astrocytes, Figure 4.18. Mainly, to understand which is the best concentration and time in culture to perform the nanoparticles-cellular studies.

EC and glioma cells have the same cell concentration density, 200000 cells/mL and it is the 2 hours curve that presents a linear curve, which indicates the best option to correlate the nanoparticles viability values. However, when astrocytes values were analyzed, it was difficult to have differences between the time and a good correlation, due to the low cell proliferation and cell quantities. Besides, this problems it was choose 24 hours and 20000 cellular initial concentration to perform the follow studies.

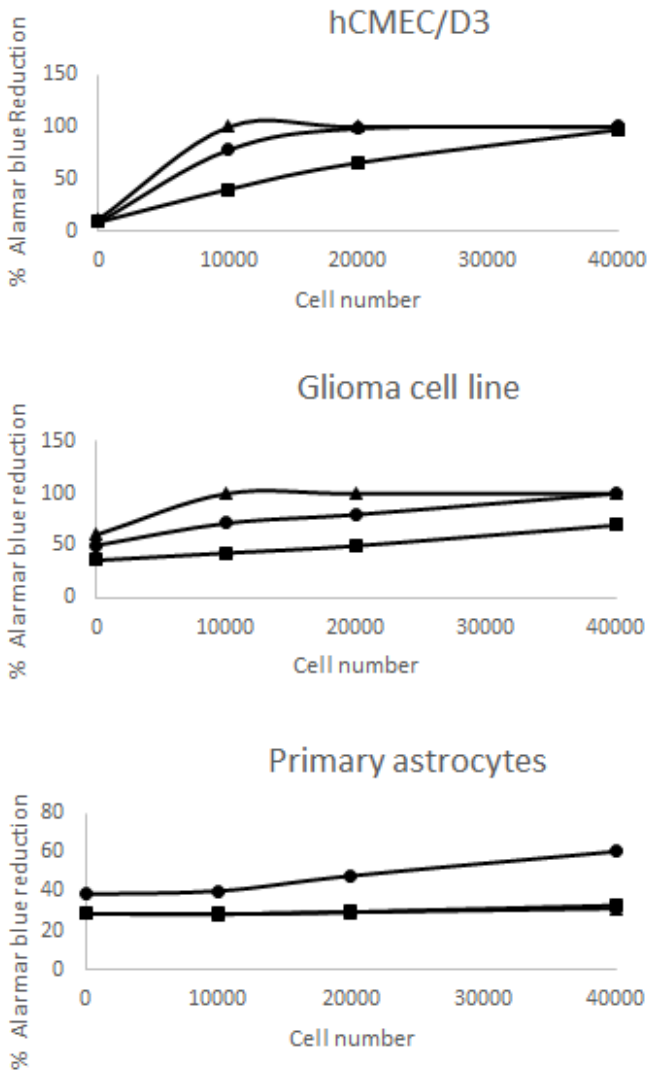


**Figure 4.18** Reduction of Alarmar blue reagent on endothelial cells, on glioma cells and primary astrocytes. The symbols —■— indicates 2h of incubation; —●— indicates 4h of incubation and —▲— indicates 24h of incubation.

Figure 4.19 shows the viability assays results using CPT free drug, SLN, CPT-SLN and as control it was used untreated cells. Firstly, the cells were seeded on the 96 well plate and incubated during 24 hours. Then, different conditions were tested and controls were established at the same time. On the next day, it was added 10% of Alarmar Blue assay in the three different cells types and in all conditions. Finally, the absorbance were measured and viability results were calculated.

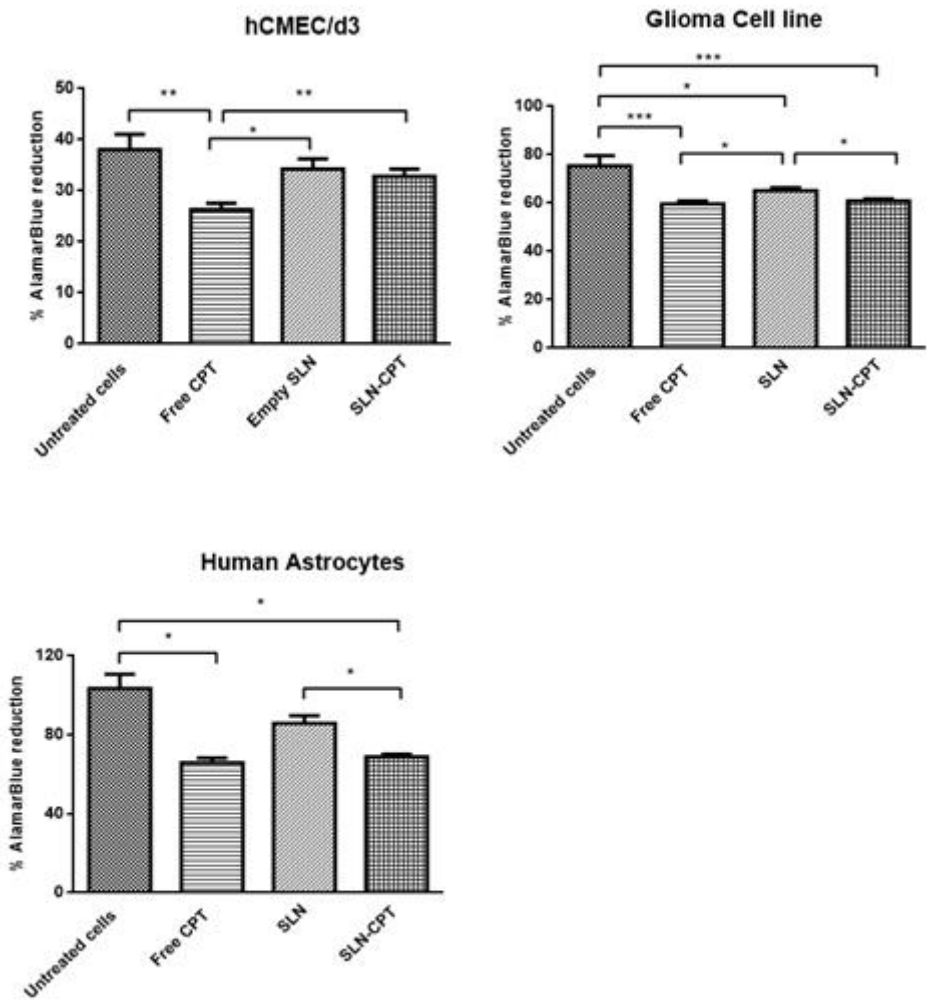


**Figure 4.19** Cellular viability of hCMEC/D3, human astrocytes and U87 cell line using the Alamar Blue Cell Viability Assay Reagent. Data is expressed as percentage of AlamarBlue reduction and represents the average of at least six independent samples. * ($p \leq 0.05$) indicates statistical significant differences; ** ($p \leq 0.01$) indicates very statistical significant differences and *** ($p \leq 0.001$) indicates extremely significant statistical differences.

In the three cellular conditions the unloaded SLN showed low cytotoxicity and presents higher cytotoxicity when CPT was incorporated in SLN. In the three cases, there are cytotoxicity associated to the free drug, however when it is loaded in the SLN this cytotoxicity is

prevented as it was expected. There are cytotoxicity associated to the unloaded SLN comparing to the untreated cells which can be the excipients used on the SLN matrix can inhibit the activity of the cells.

The hCMEC/D3 viability values of CPT formulations showed higher potency as compared to the free CPT in solution. Otherwise, viability results revealed a similar cytotoxicity to CPT-SLN and the free drug in solution. Also, it is happens with astrocytes viability results.

Comparing U87 cell line with EC with, CPT-SLN presents high cytotoxicity. This enhanced cytotoxicity of CPT-SLN can be explained by the fact that CPT-SLN can deliver more consistently. And, also, can be related to a higher uptake of camptothecin when incorporated in SLN by U87 cell line which is desired for drug efficacy in tumor brains.

Concerning to astrocytes, there are cytotoxicity associated to the SLN-CPT similar to the free drug in solution which can be explain by the cellular limitation and for the high incubation time, 24h. In order to have accurate values, it is needed to test a high initial concentration and leave them to establish for more days in the 96 well plate culture.

# Chapter 5

# Conclusion

Recently, the interest on brain diseases drugs has been increased. But, the translational to the industry remain do not happen. Principally, it is due to the difficulty to cross the BBB and the low understand in all mechanisms and interactions involved in this barrier. So the study of this barrier need to be the first step in the study of new drugs. In case of brain tumors there is no effective treatment. Even though, there are different drugs to minimize the symptoms, the real treatment is far. However, using drug loaded into nanoparticles, it is possible increase effective treatment and reduce side effects.

Taking this premises, it was purposed an *in vitro* BBB model and different techniques were applied. The monoculture model achieved on the $7^{th}$ day the higher TEER values and with $4.6x10^4$cells/$cm^2$ as initial concentration, around 32 $\Omega cm^2$. Also, immunocytochemistry using membrane markers and optical microscopy staining with GIEMSA at different days showed the monolayer growth and the cellular senescence on the last day. Moreover, at 7 day the monolayer presents a confluent monolayer. Flow cytometry and immunocytochemistry using endothelial specific markers revealed the endothelial phenotype and the confluent monolayer on $7^{th}$ day. Also, the permeability assay showed the highly restrictive barrier, since the only 24% for FD4, 11 % for FD40 and 2.56% for FD70 can be able to cross the endothelial barrier.

When, other factors were added to the *in vitro* model, there are changes on the TEER values. U87 cell line co-cultured with EC decreased TEER values around 20 $\Omega cm^2$ on $7^{th}$ day, mainly by the barrier disrupted. Astrocytes co-cultured with EC decreased TEER values to values around 25 $\Omega cm^2$, on $7^{th}$ day because of the cellular limitation. Also, on the triple co-cultured system the TEER values are lower when compared with the endothelial cell monoculture. Concerning, to permeability analysis all conditions present lower apparent permeability values than on the monoculture condition. In case of U87 cell line co-cultures with EC the

apparent permeability is around 8.9 ± 0.5x10$^{-6}$ cm/s, in astrocytes co-cultured with EC 7.6 ± 6.1x10$^{-6}$ cm/s and in the triple co-cultured model is 10.5 ± 1.1x10$^{-6}$ cm/s.

The low permeability of the U87 cell line co-culture are not in agreement with SEM images, where tight junctions are cleared disrupted, so it can be a problem of the U87 cell line were seeded on the bottom of the abluminal side. Moreover, SEM images revealed the importance of the mechanical astrocytes influence on the BBB structure and mechanisms.

hCMEC/D3 cell line is the most promising immortalized cell line, since it presents the most properties existed *in vivo*. Moreover, the EC co-cultured with astrocytoma cell line clear maintains its reproducibility and can be tested as *in vitro* pathological model that could be used as tool to screening different drugs. With exception to the models where it was included astrocytes, the application of a robustness protocol it is possible to guarantee its reproducibility.

Also, in this study it was produced and characterized CPT-SLN, based on the last work done for our group. Multivariate analysis revealed that CPT-SLN has a stable structure, mainly because of the mean size around 200 nm and low size distribution.

*In vitro* viability study on EC revealed that CPT cytotoxicity is reduced when drug is incorporated in the SLN system. Moreover, the cytotoxicity of CPT-SLN has higher potency on when compared the same effect on EC, which indicates the therapeutic efficiency.

Thus, SLN can be a promising carrier since the problems of solubility, toxicity and stability are reduced in comparison with the free drug in solution. The values are promising to perform permeability analysis.

# Chapter 6

# Future work

In future, it will be interesting the use of the *in vitro* model for other team. Mainly, to discuss the laboratory problems or difficulties which can improve, the *in vitro* model establishment.

Then, the addition of other cells such as pericytes or neurons, can improve the *in vitro* BBB model complexity and can influence nanoparticles permeation and cellular interactions. To avoid limitation of astrocytes cellular number, it can be a good solution use immortalized astrocytes.

According to nanoparticles, it will be possible decrease toxicity effects by functionalization, using a specific or overexpressed BBB receptor for example the transferrin receptor. It will be necessary to study the drug release to have a conclusion of the association efficiency value. Finally, it will be interesting to perform nanoparticle permeation using the *in vitro* model purposed.

# References


1. Gilmore, J., Yi, X., Quan, L. and Kabanov, A., *Novel nanomaterials for clinical neuroscience*. Journal of NeuroImmune Pharmacology, 2008. **3**(2): p. 83-94.

2. Goldmann, E., *Vitalfarbung am Zentralnervensytems. Beitrag zur Physio-Pathologie des Plexus choriodeus und der Hirnhaute*. Berlin, Akademie der Wissenschafte, 1913.

3. Alam, M., Beg, S., Samad, A., Baboota, S., Kohli, K., Ali, J., Ahuja, A. and Akbar, M., *Strategy for effective brain drug delivery.* European Journal of Pharmaceutical Sciences, 2010. **40**(5): p. 385-403.

4. Wilhelm, I., Fazakas, Csilla, Krizbai, Istvan A, *In vitro models of the blood-brain barrier*. Acta Neurobiol Exp (Wars), 2011. **71**(1): p. 113-28.

5. Abbott, N.J., *Blood-brain barrier structure and function and the challenges for CNS drug delivery.* Journal of inherited metabolic disease, 2013: p. 1-13.

6. Siegenthaler, J., Sohet, F. and Daneman, R., *'Sealing off the CNS': cellular and molecular regulation of blood-brain barriergenesis.* Current opinion in neurobiology, 2013. **23**(6): p. 1057-1064.

7. Cardoso, F., Brites, D. and Brito, M., *Looking at the blood-brain barrier: molecular anatomy and possible investigation approaches.* Brain research reviews, 2010. **64**(2): p. 328-363.

8. De Boer, A. and P. Gaillard, *Drug targeting to the brain.* Annual Review of Pharmacology and Toxicology, 2007. **47**: p. 323-355.

9. Naik, P. and L. Cucullo, *In vitro blood-brain barrier models: current and perspective technologies.* Jounal of Pharmaceutical Science, 2012. **101**(4): p. 1337-54.

10. Ehrlich, P., *Das Sauerstoff-Bediirfniss des Organismus.* A Hirschwald, Berlin, 1885.

11. Santaguida, S., Janigro, D., Hossain, M., Oby, E., Rapp, E. and Cucullo, L., *Side by side comparison between dynamic versus static models of blood-brain barrier in vitro: A permeability study.* Brain research, 2006. **1109**(1): p. 1-13.

12. Chen, Y.a.L., L. , *Modern methods for delivery of drugs across the blood-brain barrier*. Advanced drug delivery reviews, 2012. **64**(7): p. 640-665.

13. Abbott, N., Patabendige, A., Dolman, D., Yusof, S. and Begley, D., *Structure and function of the blood-brain barrier*. Neurobiology of disease, 2010. **37**(1): p. 13-25.

14. Cucullo, L., Hossain, M., Puvenna, V., Marchi, N. and Janigro, D., *The role of shear stress in Blood-Brain Barrier endothelial physiology*. BMC neuroscience, 2011. **12**(1): p. 40-62.

15. Cucullo, L., Couraud, P., Weksler, B., Romero, I., Hossain, M., Rapp, E. and Janigro, D., *Immortalized human brain endothelial cells and flow-based vascular modeling: a marriage of convenience for rational neurovascular studies*. Journal of Cerebral Blood Flow & Metabolism, 2007. **28**(2): p. 312-328.

16. Timpl, R., Wiedemann, H., Dedlen, V., Furthmayr, H. and Kuhn, K., *A network model for the organization of type IV collagen molecules in basement membranes*. European Journal of Biochemistry, 1981. **120**(2): p. 203-211.

17. Nag, S., *The blood-brain barrier: biology and research protocols*. Vol. 89. 2003: Springer.

18. Weiss, N., Miller, F., Cazaubon, S. and Couraud, P., *The blood-brain barrier in brain homeostasis and neurological diseases*. Biochimica et Biophysica Acta (BBA)-Biomembranes, 2009. **1788**(4): p. 842-857.

19. Ballabh, P., Braun, A. and Nedergaard, M., *The blood-brain barrier: an overview: structure, regulation, and clinical implications*. Neurobiology of disease, 2004. **16**(1): p. 1-13.

20. Barres, B., *The mystery and magic of glia: a perspective on their roles in health and disease*. Neuron, 2008. **60**(3): p. 430-440.

21. Abbott, N., Rönnbäck, L. and Hansson, E., *Astrocyte-endothelial interactions at the blood-brain barrier*. Nature Reviews Neuroscience, 2006. **7**(1): p. 41-53.

22. Choi, Y.a.K., K., *Blood-neural barrier: its diversity and coordinated cell-to-cell communication*. BMB reports, 2008. **41**(5):345-52.

23. Nagpal, K., Singh, S. and Mishra, D., *Drug targeting to brain: a systematic approach to study the factors, parameters and approaches for prediction of permeability of drugs across BBB*. Expert opinion on drug delivery, 2013. **10**(7): p. 927-955.

24. Lipinski, C., *Lead-and drug-like compounds: the rule-of-five revolution*. Drug Discovery Today: Technologies, 2004. **1**(4): p. 337-341.

25. Wolburg, H., Noell, S., Mack, A., Wolburg-Buchholz, K. and Fallier-Becker, P., *Brain endothelial cells and the glio-vascular complex*. Cell and tissue research, 2009. **335**(1): p. 75-96.

26. Pardridge, W., Eisenberg, J. and Yang, J., *Human blood-brain barrier transferrin receptor*. Metabolism, 1987. **36**(9): p. 892-895.

27. Duffy, K., Pardridge, W. and Rosenfeld, R., *Human blood-brain barrier insulin-like growth factor receptor*. Metabolism, 1988. **37**(2): p. 136-140.

28. Dehouck, B., Fenart, L., Dehouck, M., Pierce, A., Torpier, G. and Cecchelli, R., *A new function for the LDL receptor: transcytosis of LDL across the blood-brain barrier*. The Journal of cell biology, 1997. **138**(4): p. 877-889.

29. Pardridge, W.M., *Blood-brain barrier drug targeting: the future of brain drug development*. Molecular interventions, 2003. **3**(2): p. 90-105.

30. Dean, M., Y. Hamon, and G. Chimini, *The human ATP-binding cassette (ABC) transporter superfamily*. Journal of Lipid Research, 2001. **42**(7): p. 1007-1017.

31. Miller, D., *Regulation of P-glycoprotein and other ABC drug transporters at the blood-brain barrier*. Trends in pharmacological sciences, 2010. **31**(6): p. 246-254.

32. Juillerat-Jeanneret, L., *The targeted delivery of cancer drugs across the blood-brain barrier: chemical modifications of drugs or drug-nanoparticles?* Drug Discovery Today, 2008. **13**(23): p. 1099-1106.

33. Jain, K., *Role of nanotechnology in developing new therapies for diseases of the nervous system*. Nanomedicine, 2006. **1**(1): p. 9-12.

34. Markoutsa, E., Pampalakis, G., Niarakis, A., Romero, I., Weksler, B., Couraud, P. and Antimisiaris, S., *Uptake and permeability studies of BBB-targeting immunoliposomes using the hCMEC/D3 cell line*. European Journal of Pharmaceutics and Biopharmaceutics, 2011. **77**(2): p. 265-274.

35. Martins, S., Sarmento, B., Nunes, C., Lúcio, M., Reis, S. and Ferreira, D., *Brain targeting effect of camptothecin-loaded solid lipid nanoparticles in rat after intravenous administration*. European Journal of Pharmaceutics and Biopharmaceutics, 2013. **85**(3): p. 488-502.

36. Wohlfart, S., Gelperina, S. and Kreuter, J., *Transport of drugs across the blood-brain barrier by nanoparticles*. Journal of Controlled Release, 2012. **161**(2): p. 264-273.

37. Gabathuler, R., *Approaches to transport therapeutic drugs across the blood-brain barrier to treat brain diseases*. Neurobiology of disease, 2010. **37**(1): p. 48-57.

38. Hervé, F., N. Ghinea, and J.-M. Scherrmann, *CNS delivery via adsorptive transcytosis*. The AAPS journal, 2008. **10**(3): p. 455-472.

39. Liu, L., Guo, K., Lu, J., Venkatraman, S., Luo, D., Ng, K., Ling, E., Moochhala, S. and Yang, Y., *Biologically active core/shell nanoparticles self-assembled from cholesterol-terminated PEG-TAT for drug delivery across the blood-brain barrier*. Biomaterials, 2008. **29**(10): p. 1509-1517.

40. Pardridge, W., *The blood-brain barrier: bottleneck in brain drug development*. NeuroRx, 2005. **2**(1): p. 3-14.

41. Huynh, G., Deen, D. and Szoka Jr, F., *Barriers to carrier mediated drug and gene delivery to brain tumors*. Journal of Controlled Release, 2006. **110**(2): p. 236-259.

42. Booth, R.a.K., H., *Characterization of a microfluidic in vitro model of the blood-brain barrier* Lab on a chip, 2012. **12**(10): p. 1784-1792.

43. Ribeiro, M., Castanho, M. and Serrano, . *In Vitro Blood-Brain Barrier Models-Latest Advances and Therapeutic Applications in a Chronological Perspective*. Mini reviews in medicinal chemistry, 2010. **10**(3): p. 263-271.

44. Zhang, Z., McGoron, A., Crumpler, E. and Li, C., *Co-culture based blood-brain barrier in vitro model, a tissue engineering approach using immortalized cell lines for drug transport study*. Applied biochemistry and biotechnology, 2011. **163**(2): p. 278-295.

45. Patabendige, A., Skinner, R., Morgan, L. and Abbott, N., *A detailed method for preparation of a functional and flexible blood-brain barrier model using porcine brain endothelial cells*. Brain research, 2013. **1521**: p. 16-30.

46. Neuhaus, W., Plattner, V., Wirth, M., Germann, B., Lachmann, B., Gabor, F. and Noe, C., *Validation of in vitro cell culture models of the blood-brain barrier: tightness characterization of two promising cell lines.* Journal of pharmaceutical sciences, 2008. **97**(12): p. 5158-5175.

47. Li, G., Simon, M., Cancel, L., Shi, Z., Ji, X., Tarbell, J., Morrison III, B. and Fu, B., *Permeability of endothelial and astrocyte cocultures: in vitro blood-brain barrier models for drug delivery studies.* Annals of biomedical engineering, 2010. **38**(8): p. 2499-2511.

48. Weksler, B., Romero, I. and Couraud, P., *The hCMEC/D3 cell line as a model of the human blood brain barrier.* Fluids Barriers CNS, 2013. **10**(1): p. 16-26.

49. Hatherell, K., Couraud, P., Romero, I., Weksler, B. and Pilkington, G., *Development of a three-dimensional, all-human in vitro model of the blood-brain barrier using mono-, co-, and tri-cultivation Transwell models.* Journal of neuroscience methods, 2011. **199**(2): p. 223-229.

50. Ong, S., Zhao, Z., Arooz, T., Zhao, D., Zhang, S., Du, T., Wasser, M., van Noort, D., Yu, H., *Engineering a scaffold-free 3D tumor model for< i> in vitro</i> drug penetration studies.* Biomaterials, 2010. **31**(6): p. 1180-1190.

51. Ogunshola, O., *In vitro modeling of the blood-brain barrier: simplicity versus complexity.* Current pharmaceutical design, 2011. **17**(26): p. 2755-2761.

52. Bussolari, S.R., C.F. Dewey, and M.A. Gimbrone, *Apparatus for subjecting living cells to fluid shear stress.* Review of Scientific Instruments, 1982. **53**(12): p. 1851-1854.

53. Griep, L., Wolbers, F., de Wagenaar, B. ter Braak, P., Weksler, B. Romero, I., Couraud, P., Vermes, I., van der Meer, A. and van den Berg, A., *BBB ON CHIP: microfluidic platform to mechanically and biochemically modulate blood-brain barrier function.* Biomedical microdevices, 2013. **15**(1): p. 145-150.

54. Weksler, B., Subileau, E., Perriere, N., Charneau, P., Holloway, K., Leveque, M., Tricoire-Leignel, H., Nicotra, A., Bourdoulous, S. and Turowski, P., *Blood-brain barrier-specific properties of a human adult brain endothelial cell line.* The Federation American Societies Experimental Biology journal, 2005. **19**(13): p. 1872-1874.

55. Wong, A., Ye, M., Levy, A., Rothstein, J., Bergles, D. and Searson, P., *The blood-brain barrier: an engineering perspective.* Frontiers in neuroengineering, 2013. **6**: p. 7-30.

56. Martins, S., Wendling, T., Gonçalves, V., Sarmento, B. and Ferreira, D., *Development and validation of a simple reversed-phase HPLC method for the determination of camptothecin in animal organs following administration in solid lipid nanoparticles.* Journal of Chromatography. B, Analytical technologies in the biomedical and life sciences, 2012. **880**(1): p. 100-107.

57. Martins, S., Tho, I., Souto, E., Ferreira, D. and Brandl, M., *Multivariate design for the evaluation of lipid and surfactant composition effect for optimisation of lipid nanoparticles.* European Journal of Pharmaceutical Sciences, 2012. **45**(5): p. 613-623.

58. Das, S., Ng, W. and Tan, R., *Sucrose ester stabilized solid lipid nanoparticles and nanostructured lipid carriers: I. Effect of formulation variables on the physicochemical properties, drug release and stability of clotrimazole-loaded nanoparticles.* Nanotechnology, 2014. **25**(10): p. 105101.

59. Rahier, N., Eisenhauer, B., Gao, R., Jones, S. and Hecht, S., *Water-soluble camptothecin derivatives that are intrinsic topoisomerase I poisons*. Organic letters, 2004. **6**(3): p. 321-324.

60. Ragnaill, M., Brown, M., Ye, D., Bramini, M., Callanan, S., Lynch, I. and Dawson, K., *Internal benchmarking of a human blood-brain barrier cell model for screening of nanoparticle uptake and transcytosis*. European Journal of Pharmaceutics and Biopharmaceutics, 2011. **77**(3): p. 360-367.

61. Czupalla, C., Liebner, S. and Devraj, K., *In Vitro Models of the Blood-Brain Barrier*, in *Cerebral Angiogenesis*. 2014, Springer. p. 415-437.

62. Förster, C., Burek, M., Romero, I., Weksler, B., Couraud, P. and Drenckhahn, D., *Differential effects of hydrocortisone and TNFa on tight junction proteins in an in vitro model of the human blood-brain barrier*. The Journal of physiology, 2008. **586**(7): p. 1937-1949.

63. Urich, E., Lazic, S., Molnos, J., Wells, I. and Freskgård, P., *Transcriptional profiling of human brain endothelial cells reveals key properties crucial for predictive in vitro blood-brain barrier models*. PloS one, 2012. **7**(5): p. e38149.

64. Paolinelli, R., et al., *Wnt activation of immortalized brain endothelial cells as a tool for generating a standardized model of the blood brain barrier in vitro*. PloS one, 2013. **8**(8): p. e70233.

65. Khodarev, N., Yu, J., Labay, E., Darga, T., Brown, C., Mauceri, H., Yassari, R., Gupta, N. and Weichselbaum, R., *Tumour-endothelium interactions in co-culture: coordinated changes of gene expression profiles and phenotypic properties of endothelial cells*. Journal of cell science, 2003. **116**(6): p. 1013-1022.

66. Dwyer, J., Hebda, J., Le Guelte, A., Galan-Moya, E., Smith, S., Azzi, S., Bidere, N. and Gavard, J., *Glioblastoma cell-secreted interleukin-8 induces brain endothelial cell permeability via CXCR2*. PloS one, 2012. **7**(9): p. e45562.

67. Poller, B., Gutmann, H., Krähenbühl, S., Weksler, B., Romero, I., Couraud, P., Tuffin, G., Drewe, J. and Huwyler, J., *The human brain endothelial cell line hCMEC/D3 as a human blood-brain barrier model for drug transport studies*. Journal of Neurochemistry, 2008. **107**(5): p. 1358-1368.

68. Hayashi, Y., Nomura, M., Yamagishi, S., Harada, S., Yamashita, J., and Yamamoto, H., *Induction of various blood-brain barrier properties in non-neural endothelial cells by close apposition to co-cultured astrocytes*. Glia, 1997. **19**(1): p. 13-26.